
JacQuant: STE-Free Quantization-Aware Training via Learned Jacobian Surrogates

Kai Yi*
Meta AI

Vignesh Vivekraj
Meta AI

Harshit Khaitan
Meta AI

Steven Li
Meta AI

Abstract

Quantization-aware training (QAT) is widely deployed but typically relies on the Straight-Through Estimator (STE), which passes gradients through non-differentiable quantizers by fiat. This often makes training brittle near bin boundaries and weakly aligned with the actual behavior of the low-precision model. We introduce JacQuant, a QAT framework that learns a lightweight surrogate of the model’s local sensitivity to parameter changes and uses it to stabilize and accelerate training within standard variance-reduced optimizers. The surrogate is inexpensive (diagonal or block-diagonal), data-driven, and compatible with common weight and activation quantizers. On “code-preserving” training phases, we prove convergence for non-convex objectives and obtain linear rates under a PL condition, and we relate the learned sensitivity to end-to-end output fidelity via a simple calibration argument. Across LLM benchmarks at ≤ 2 bits, JacQuant consistently reaches higher accuracy than STE-based QAT, and the runtime analyses on various models show that the added cost remains negligible under practical group sizes. The method is drop-in and requires no changes to the forward quantizers; our empirical claims are scoped to ultra-low-bit LLM QAT.

1 Introduction

Quantization is a primary route to deploy large language models (LLMs) under tight memory and latency budgets by reducing parameter precision and improving hardware utilization (Egiazarian et al., 2024; Frantar et al., 2023; Tseng et al., 2024; Liu et al., 2024, 2025b). In many practical deployments, *post-training quantization* (PTQ) remains attractive because it avoids gradient-based training and can be applied quickly to a pretrained checkpoint (Frantar et al., 2023; Tseng et al., 2024). However, when pushing to *ultra-low precision*, most notably ≤ 2 -bit weights, PTQ often suffers sharp degradation, and *quantization-aware training* (QAT) becomes important to recover accuracy by adapting scales, clipping, and representations to the task distribution (Liu et al., 2025b; Li et al., 2026).

Almost all modern QAT relies on the *Straight-Through Estimator* (STE) (Bengio et al., 2013): the forward pass uses a hard quantizer $Q_{\Delta}(\cdot)$, but backpropagation pretends its Jacobian is the identity. This creates a persistent mismatch because hard quantizers are piecewise constant and dominated by bin boundaries and saturation/clipping at low bit-widths (Yin et al., 2019; Esser et al., 2020; Nagel et al., 2020). In the ≤ 2 -bit regime, where many parameters lie near boundaries or hit clipping limits, STE’s identity Jacobian can over-propagate gradients, leading to instability and suboptimal solutions.

Key idea: *learn the missing quantizer Jacobian.* We view QAT as a *missing-Jacobian* problem and introduce JacQuant (Jacobian learning for Quantization), which keeps the *deployed hard quantizer* in the forward pass but replaces STE’s fixed identity Jacobian with a learned surrogate sensitivity map $B(W)$. Let $q = Q_{\Delta}(W)$ and $v = \nabla_{q\ell}$. JacQuant uses $\nabla_{W\ell} \approx B(W)v$, where $B(W)$ is diagonal

*Correspondence to: kaiyi96@meta.com.

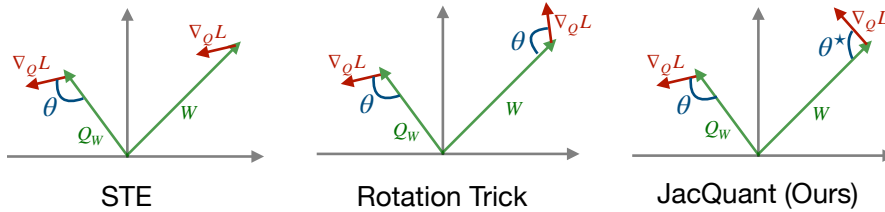


Figure 1: Gradient propagation schemes in quantized optimization. *Left*: STE, which directly copies the forward gradient direction. *Middle*: Rotation Trick (Fifty et al., 2025), which applies a fixed relative rotation θ to the gradient. *Right*: JacQuant (ours), which learns an adaptive surrogate Jacobian $B(W)$, yielding an optimal rotation θ^* together with an optimal gradient rescaling.

or block-diagonal with one scalar per quantization group, making it cheap and easy to integrate. We train $B(W)$ to track the quantizer’s *local sensitivity*: near 1 in bin interiors and near 0 under active saturation, producing geometry-aware gradients that naturally damp saturated directions and reduce oscillations near boundaries.

In Fig. 1, we contrast our approach with representative prior methods. STE treats quantization as gradient-transparent; fixed-transform methods (e.g., Rotation Trick (Fifty et al., 2025)) alter gradient geometry in a static way. In contrast, JacQuant learns an *adaptive* backward gain $B(W)$ that aligns gradient propagation with how the hard quantizer actually responds to perturbations, especially under clipping/saturation where STE is most misaligned.

To keep the additional cost negligible, JacQuant updates the surrogate Jacobian $B(W)$ only occasionally and amortizes it across many QAT steps. Sensitivity is estimated using either random *probes* or *subtractive dithering*, requiring only a single scalar per group and preserving standard QAT throughput. While the framework is compatible with classical variance-reduction or control-variate techniques, the central departure from STE lies in explicitly learning the Jacobian rather than assuming an identity surrogate.

Our **contributions** are summarized as follows:

- *STE-free backward rule via Jacobian learning*: we replace STE’s identity Jacobian with a learned, group-wise sensitivity map $B(W)$ while keeping the hard forward quantizer unchanged.
- *Practical estimators with negligible overhead*. We propose two efficient estimators (Probe and Dither) that update $B(W)$ intermittently and scale naturally with group-wise quantization.
- *Theory for a principled target gradient*. Using a smoothed/dithered quantization model, we relate JacQuant’s updates to a well-defined target gradient and establish standard non-convex convergence guarantees (and linear rates under a PL condition) when $B(W)$ tracks the mean sensitivity (Karimi et al., 2016).
- *Extensive empirical validation on LLMs*. We demonstrate that JacQuant is a drop-in upgrade to STE-based QAT pipelines and improves stability and accuracy in ≤ 2 -bit regimes on LLM benchmarks. Empirically, we evaluate JacQuant on LLaMA3-1B/3B, Qwen3-1.7B, and a LLaMA3-8B W2A16 trajectory; compare against Rotation Trick under matched ParetoQ settings; and report runtime overhead on both LLaMA3-1B and LLaMA3-8B. We scope the empirical claim to ultra-low-bit LLM QAT while isolating the algorithmic contribution to the backward rule.

2 Related Work

Post-training quantization (PTQ). PTQ calibrates a pretrained model without gradient updates and remains a strong default for rapid LLM deployment. Representative methods include SmoothQuant (Xiao et al., 2023) (activation outlier smoothing for W8A8), GPTQ (Frantar et al., 2023) (Hessian-informed weight-only quantization), ZeroQuant/ZeroQuant-V2 (Yao et al., 2022, 2023) (per-layer PTQ with hardware-friendly kernels), and AWQ (Lin et al., 2024) (activation-aware protection of salient channels for 4-bit inference).

Quantization-aware training (QAT). QAT typically improves accuracy in aggressive regimes (e.g., ≤ 2 -bit weights and/or W&A quantization) by adapting scales and clipping to the task distribution

rather than relying purely on calibration statistics. Classic STE-based QAT spans early work such as DoReFa-Net (Zhou et al., 2016), PACT (Choi et al., 2018), and step-size learning methods such as LSQ/LSQ+ (Esser et al., 2020; Bhalgat et al., 2020). Recent findings similarly suggest QAT is often preferable to PTQ in ultra-low-bit settings (e.g., ParetoQ (Liu et al., 2025b), WinQ (Li et al., 2026)).

Beyond the Straight-Through Estimator. Most QAT methods propagate gradients through quantizers using the Straight-Through Estimator (STE), which can be biased near bin boundaries and poorly aligned with the true low-precision objective. Two notable departures are PV-Tuning (Malinovskii et al., 2024), which uses a proximal surrogate, and the Rotation Trick (Fifty et al., 2025), which applies a fixed geometric alignment. Other complementary routes include differentiable relaxations/annealing (e.g., Soft-to-Hard VQ (Agustsson et al., 2017)) and hybrid first/zeroth-order corrections (e.g., FOGZO (Yang & Aamodt, 2025)), as well as optimizer-level advances (e.g., Muon (Liu et al., 2025a)). Zeroth-order approaches such as ZeroQAT (Tan et al., 2025) address a complementary cost regime: they change the gradient-estimation mechanism, whereas JacQuant isolates the backward rule through the deployed hard quantizer and amortizes probing cost across many QAT steps. We pursue *Jacobian learning* because it preserves the deployed hard quantizer in the forward pass, yet replaces the fixed STE with a lightweight learned sensitivity map $B(W)$ that (i) *reduces bias* by matching local quantization sensitivity, (ii) *stabilizes* training via adaptive damping near saturation/clipping, and (iii) amortizes any probing cost by updating $B(W)$ only occasionally. An expanded comparison is provided in Sec. C.2.

Variance reduction. Control-variate methods (e.g., SAG (Roux et al., 2012), SVRG (Johnson & Zhang, 2013), SAGA (Defazio et al., 2014)) and Jacobian-sketching (JacSketch (Gower et al., 2021)) reduce stochastic noise in large-scale optimization. We adapt these ideas to stabilize Jacobian-modulated QAT updates with minimal overhead; see Sec. C.3 and D.

3 Method

We introduce JacQuant, a QAT framework that replaces STE with a *learned surrogate Jacobian*. Rather than treating quantization as “identity in backward”, we learn how perturbations of full-precision weights *affect* their quantized proxies and use this sensitivity to map gradients back to weight space.

3.1 Preliminaries: Grouped Quantization in LLMs

Consider a linear layer with weights $W \in \mathbb{R}^{d_{\text{out}} \times d_{\text{in}}}$ and input x , producing $z = Wx$. QAT uses a quantized proxy $\widehat{W} = Q_{\Delta}(W)$ in the forward pass. We use *grouped quantization*: partition weights into groups $\{W^{(g)}\}_{g=1}^G$ (e.g., 128 weights per group) and quantize each group independently. For a sample (x_i, y_i) , let $v_i := \nabla_{\widehat{W}} \ell(f(x_i; \widehat{W}), y_i)|_{\widehat{W}=Q_{\Delta}(W)}$. The challenge is that $Q_{\Delta}(\cdot)$ is piecewise constant (often with clipping), so its true Jacobian is missing.

3.2 The Core Idea: Learning the Quantization Jacobian

We optimize the standard supervised objective

$$L(W) = \mathbb{E}_{(x,y) \sim \mathcal{D}} [\ell(f(x; Q_{\Delta}(W)), y)]. \quad (1)$$

STE corresponds to using an identity surrogate for the missing Jacobian. JacQuant instead learns a lightweight sensitivity map $B(W)$ and uses the backward rule

$$\nabla_W L(W) \approx B(W) \nabla_{\widehat{W}} L(\widehat{W})|_{\widehat{W}=Q_{\Delta}(W)}. \quad (2)$$

Parameterization and cost. We use a block-diagonal $B(W)$ with one scalar per quantization group, $B(W) = \text{blkdiag}(b_1 I, \dots, b_G I)$. With group size 128 this adds one scalar per 128 weights (negligible vs. optimizer state).

Algorithm 1 JacQuant-VR (unified view)

Require: W_0 , dataset \mathcal{D} , quantizer Q_Δ , stepsize η , refresh prob $p \in (0, 1]$, mode $\in \{\text{PROBE}, \text{DITHER}\}$, EMA rate β

- 1: $B_0 \leftarrow I$; anchors $(\tilde{W}, \tilde{B}) \leftarrow (W_0, B_0)$ ▷ start from the STE gain
- 2: VR state s_0 ; reference gradient $\tilde{g} \leftarrow \text{REFGRAD}(\tilde{W}, \tilde{B})$ ▷ anchor/control variate
- 3: **for** $t = 0, 1, \dots$ **do**
- 4: Sample minibatch $S_t \subset \mathcal{D}$
- 5: $g_t \leftarrow \text{GRADEST}(W_t, B_t, \tilde{W}, \tilde{B}, \tilde{g}, s_t; S_t)$ ▷ backprop uses learned B_t
- 6: $W_{t+1} \leftarrow W_t - \eta g_t$ ▷ standard QAT update
- 7: $s_{t+1} \leftarrow \text{CTRLUPDATE}(s_t, W_{t+1}, \tilde{W}; S_t)$ ▷ update VR memory if used
- 8: **if** $u \sim \text{Unif}[0, 1] \leq p$ (or criterion \mathcal{C} holds) **then** ▷ refresh rarely
- 9: **if** PROBE **then**
- 10: $B_{t+1} \leftarrow (1-\beta)B_t + \beta \text{PROBEUPDATE}(W_{t+1})$ ▷ fit local slope
- 11: **else**
- 12: $B_{t+1} \leftarrow (1-\beta)B_t + \beta \text{DITHERUPDATE}(W_{t+1})$ ▷ dithered sensitivity
- 13: **end if**
- 14: $(\tilde{W}, \tilde{B}) \leftarrow (W_{t+1}, B_{t+1})$ ▷ synchronize anchor
- 15: $\tilde{g} \leftarrow \text{REFGRAD}(\tilde{W}, \tilde{B})$ ▷ refresh reference
- 16: **else**
- 17: $B_{t+1} \leftarrow B_t$ ▷ reuse amortized Jacobian
- 18: **end if**
- 19: **end for**

3.3 Practical Estimation of $B(W)$

JacQuant updates $B(W)$ only on refresh steps (Alg. 1) and reuses it across many QAT iterations.

JacQuant-Probe (default). For each group g , draw $\delta_g \sim \mathcal{N}(0, \sigma^2 I)$ and measure $\Delta q_g = Q_\Delta(W_g + \delta_g) - Q_\Delta(W_g)$. A one-step slope fit gives

$$\hat{b}_g = \frac{\langle \Delta q_g, \delta_g \rangle}{\|\delta_g\|_2^2 + \epsilon}, \quad b_g \leftarrow (1 - \beta)b_g + \beta \text{clip}(\hat{b}_g, 0, 1). \quad (3)$$

JacQuant-Dither. We also consider subtractive dithering $r_g \sim \mathcal{U}[-\Delta/2, \Delta/2]$ and the de-dithered proxy $q_g = Q_\Delta(W_g + r_g) - r_g$, and update b_g toward the empirical sensitivity of $W_g \mapsto q_g$. We provide the full estimator and implementation details in [Secs. C.3](#) and [D](#).

3.4 Optional Variance Reduction

Jacobian learning adds stochasticity (from probes/dithers), so JacQuant can be combined with scalable variance-reduced estimators via occasional refresh steps (Alg. 1). [Sec. C.3](#) gives the concrete control-variate forms. Disabling the control-variate state yields JacQuant-Base (Alg. 3), isolating the effect of Jacobian learning.

4 Convergence Analysis of JacQuant

Analytical storyline. The analysis is organized around one question: *what should replace the identity Jacobian used by STE, and what happens to optimization when we use this replacement?* The argument has four linked parts. First, because a hard quantizer is piecewise constant, we analyze short *code-preserving windows* and introduce a smoothed reference gradient that has a well-defined quantizer sensitivity $J(W)$. Second, we show that the only extra bias in JacQuant is the mismatch $B(W) - J(W)$, whereas STE has the fixed mismatch $I - J(W)$. Third, we prove that the probe and dither updates estimate this same $J(W)$ and therefore make the learned backward map competitive with, and often less biased than, STE. Finally, once this surrogate gradient is bounded and locally regular, standard stochastic/variance-reduced convergence rates apply with two interpretable residuals: a Jacobian-tracking bias and a stochastic-variance floor. Thus the proof should be read as a chain rather than a list of independent claims: [Lem. 1](#) defines the target that STE misses, [Lems. 2](#) and [3](#) and [Prop. 1](#) explain how the algorithm learns that target, and [Lems. 4](#) and [6](#) and [Thms. 1](#) and [2](#) show that optimization behaves like a standard smooth stochastic method once the remaining Jacobian error and variance are accounted for.

4.1 Local Smoothness and the Target Gradient

Quantization $Q_\Delta : \mathbb{R}^d \rightarrow \mathbb{R}^d$ has derivative zero almost everywhere and undefined derivative on cell boundaries. Directly analyzing $\nabla_W L(Q_\Delta(W))$ is therefore uninformative. We instead examine short intervals during training in which the quantization code does not change. This assumption is not an algorithmic restriction; it is a local analytical device matching the practical fact that QAT weights usually cross quantization cells only intermittently.

Assumption 1 (Code preservation). There exist t_0 and $T \geq 1$ such that $Q_\Delta(W_t) = Q_\Delta(W_{t_0}) \equiv q$ for all $t \in [t_0, t_0 + T)$.

Within such a window, let $v_i := \nabla_q \ell(f(x_i; q), y_i)$ and $\bar{v} := n^{-1} \sum_i v_i$. To define a meaningful gradient through the hard quantizer, we smooth the quantizer by subtractive dithering:

$$m(W) := \mathbb{E}_r[Q_\Delta(W + r) - r], \quad r \sim \text{Unif}[-\Delta/2, \Delta/2],$$

and define the mean-field quantizer sensitivity $J(W) := \nabla_W m(W)$. For unclipped bin interiors, $J(W)$ is close to the identity; near clipping or saturation, its diagonal entries shrink toward zero. Thus the principled target gradient is

$$g^\dagger(W) = J(W)\bar{v},$$

which is the gradient of the dither-averaged quantized objective on the window. JacQuant uses $g_B(W) = B(W)\bar{v}$, whereas STE uses $g^{\text{STE}}(W) = \bar{v}$.

Lemma 1 (Bias to the target gradient). *On a code-preserving window,*

$$\|g_B(W) - g^\dagger(W)\| \leq \|B(W) - J(W)\| \|\bar{v}\|, \quad \|g^{\text{STE}}(W) - g^\dagger(W)\| \leq \|I - J(W)\| \|\bar{v}\|.$$

Why this lemma is the core comparison. The lemma isolates the backward-rule question from all other parts of QAT. If a coordinate is in a stable bin interior, $J(W) \approx I$ and STE is already reasonable; JacQuant is designed to recover the same behavior because $B(W)$ is initialized/updated toward identity-like sensitivity there. The difference appears near clipping and saturation, where $J(W) \preceq I$ and STE still transmits the full upstream gradient. In that regime, learning $B(W) \approx J(W)$ produces the desired damping and directly reduces the target-gradient bias.

4.2 Why the Learned $B(W)$ Tracks $J(W)$

The previous lemma is useful only if $B(W)$ can actually approach $J(W)$. The next results explain this in the same order as the algorithm: probing estimates a local slope, the EMA recursion tracks the slowly moving target, and dithering gives an alternative estimator with the same population fixed point. This connects directly to the refresh block of [Alg. 1](#): each refresh obtains a noisy measurement of local quantizer response, while the EMA prevents that measurement noise from becoming a high-frequency change in the backward rule.

Lemma 2 (Probe-LS consistency on a fixed window). *Fix a code-preserving window and a group g of size d_g . Draw m i.i.d. probes $\delta_k \sim \mathcal{N}(0, \sigma^2 I)$ and observe $\Delta q_k = Q_\Delta(W + \delta_k) - Q_\Delta(W)$. Let \hat{B}_g minimize $\sum_{k=1}^m \|\Delta q_{g,k} - B_g \delta_{g,k}\|^2$ over the diagonal or block-diagonal class used by JacQuant. Then, for a universal constant C and any $\delta \in (0, 1)$,*

$$\Pr \left(\|\hat{B}_g - J_g(W)\| \leq C\sigma^{-1} \sqrt{\frac{d_g + \log(1/\delta)}{m}} \right) \geq 1 - \delta.$$

What the probe lemma says. The probe update is not an arbitrary learned gate: it is a local regression of quantized output changes Δq on weight perturbations δ . On a fixed window, the cross-moment relation $\mathbb{E}[\Delta q \delta^\top] = J(W)\mathbb{E}[\delta \delta^\top]$ makes the least-squares target equal to the mean-field sensitivity. The bound also explains the group-size trade-off seen in ablations: finer groups can represent more heterogeneous sensitivity, but they require more reliable slope estimates; overly noisy estimates inject unnecessary backward-rule variance.

Proposition 1 (EMA/SA tracking with drifting W). *Under Robbins–Monro stepsizes, persistent probe excitation, compact projection of B_t , and slower drift of W_t , the EMA recursion for B_t satisfies*

$$\mathbb{E}[\|B_{t+1} - J(W_t)\| \mid \mathcal{F}_t] \leq \rho \|B_t - J(W_t)\| + \zeta_t,$$

for some $0 < \rho < 1$ and $\zeta_t \rightarrow 0$. Hence B_t tracks $J(W_t)$ in probability, and almost surely when the drift errors are summable.

Why tracking matters. The static probe estimate would be insufficient if the target sensitivity changed too quickly. The proposition states the needed separation of time scales: QAT updates move the weights, but B_t is refreshed often enough, and with enough excitation, to follow the moving mean-field sensitivity. This justifies amortizing the Jacobian updates over many training steps instead of re-estimating them every iteration.

Lemma 3 (Dither fixed point equals $J(W)$). *With uniform subtractive dithering, $J(W) = \nabla_W \mathbb{E}_r [Q_\Delta(W + r) - r]$ is the unique population fixed point of the dither-induced update on a code-preserving window.*

Role of the dither lemma. Probe and dither use different measurements, but they target the same object. Dithering randomizes thresholds so that the expected hard quantizer becomes differentiable; its derivative is exactly the desired mean-field sensitivity. Therefore the two practical estimators are not separate heuristics, but two ways of learning the same missing Jacobian.

Corollary 1 (Data-driven dominance over STE). *Let $\gamma(W_t) := \|I - J(W_t)\|$. If, after tracking, $\|B_t - J(W_t)\| \leq \gamma(W_t) - \epsilon$, then*

$$\|g_{B_t}(W_t) - g^\dagger(W_t)\| \leq \|g^{\text{STE}}(W_t) - g^\dagger(W_t)\| - \epsilon \|\bar{v}_t\|.$$

Interpretation. The corollary turns the tracking results into the practical claim: once B_t is closer to $J(W_t)$ than the identity is, JacQuant has a strictly smaller bias to the smoothed target gradient. In bin interiors, $\gamma(W_t)$ is small and JacQuant should behave similarly to STE; near saturation, $\gamma(W_t)$ is large and the learned damping can provide a meaningful advantage. This is the point where the analysis links back to the observed training behavior: JacQuant does not need to change the hard forward quantizer; it only changes how much upstream gradient is trusted in groups where the forward quantizer is locally insensitive.

4.3 Stability of the Surrogate Gradient

Bias reduction alone is not enough; the surrogate direction must also be stable enough for stochastic optimization. We impose a mild regularity condition that matches the implemented diagonal/block-diagonal parameterization with clipping of group gains.

Assumption 2 (Boundedness and regularity of B). $B(W)$ is diagonal or block-diagonal, uniformly bounded as $\|B(W)\| \leq \beta_B$, and locally Lipschitz on each code-preserving window.

Lemma 4 (Spectral stability). *Under Assump. 2, $\|B(W)v_i\| \leq \beta_B \|v_i\|$ for every per-example backpropagation signal v_i . When the learned sensitivity tracks clipping/saturation with gain below one, it damps directions that STE would transmit unchanged.*

Why this is not just a boundedness lemma. The learned Jacobian acts as an automatic gain controller. Its gain remains close to one where the quantizer is locally responsive, but drops in regions where the quantized forward map is insensitive. This is precisely the ‘‘saturation damping’’ effect: the backward pass no longer pushes hard in directions where the forward quantizer cannot respond proportionally.

Lemma 5 (Local Lipschitzness). *On a fixed code assignment, $F_i(W) = B(W)v_i$ is locally Lipschitz, and the corresponding windowed surrogate dynamics satisfy the smoothness conditions required by the descent analysis.*

How this connects to convergence. Lems. 4 and 5 convert the discontinuous training problem into a locally smooth surrogate problem for the purpose of analyzing updates. The discontinuity is still present in the forward pass, but the backward directions used inside a window are bounded, regular, and aligned with the mean-field sensitivity.

4.4 Windowed and End-to-End Rates

Let the stochastic/variance-reduced estimator be

$$g_t = \text{GradEst}(W_t, B_t, \tilde{W}, \tilde{B}, \tilde{g}, s_t; S_t), \quad (4)$$

where $(\tilde{W}, \tilde{B}, \tilde{g})$ is an occasionally refreshed anchor state. The proof uses the following standard ABC-style oracle bound, which covers the loopless-SVRG/control-variate form used in JacQuant

while keeping the theorem independent of a particular implementation. At this stage the discontinuous-quantizer issue has been reduced to an imperfect-oracle issue: the estimator may be biased by $B_t - J(W_t)$ and noisy because of minibatches/anchors, and the convergence rates track exactly these two quantities.

Assumption 3 (JacQuant-VR with general bounds). There is a nonnegative state-variance proxy σ_t and constants $A, B, C, \tilde{A}, \tilde{B}, \tilde{C} \geq 0$ with $\tilde{B} < 1$ such that, on a code-preserving window,

$$\mathbb{E}[\|g_t - \nabla \tilde{L}(W_t)\|^2 \mid \mathcal{F}_t] \leq 2A(\tilde{L}(W_t) - \tilde{L}^*) + B\sigma_t + C, \quad (\text{ABC-1})$$

$$\mathbb{E}[\sigma_{t+1} \mid \mathcal{F}_t] \leq 2\tilde{A}(\tilde{L}(W_t) - \tilde{L}^*) + \tilde{B}\sigma_t + \tilde{C}. \quad (\text{ABC-2})$$

The anchor/reference gradient has bounded staleness and contributes an effective variance constant $\rho\sigma_{\text{vr}}^2$ with $\rho \in (0, 1]$.

Lemma 6 (Bias/variance decomposition under VR). *Under Assump. 3, the estimator error decomposes as*

$$\mathbb{E}\|g_t - \nabla \tilde{L}(W_t)\|^2 \leq O(\|B_t - J(W_t)\|^2 \|\bar{v}_t\|^2) + O(\rho\sigma_{\text{vr}}^2).$$

Meaning of the decomposition. The first term is the Jacobian-learning error already identified in Lem. 1; it vanishes as B_t tracks $J(W_t)$. The second term is the ordinary stochastic-optimization variance after control-variate/anchor reduction. Thus VR tightens constants, while the learned Jacobian corrects the bias caused by the hard quantizer.

Theorem 1 (Non-convex windowed convergence). *Under Assumps. 1 to 3 and L_s -smoothness on the window, for $\eta \leq c/L_s$,*

$$\min_{0 \leq t < T} \mathbb{E}\|\nabla \tilde{L}(W_t)\|^2 \leq O(1/(\eta T)) + O(\varepsilon^2) + O(\rho\sigma_{\text{vr}}^2\eta), \quad \varepsilon := \sup_t \mathbb{E}\|B_t - J(W_t)\| \|\bar{v}_t\|.$$

Interpretation. The rate has the classical $O(1/T)$ stationarity term plus two transparent residuals. The $O(\varepsilon^2)$ term measures how much the learned backward map still deviates from the mean-field quantizer sensitivity; the $O(\rho\sigma_{\text{vr}}^2\eta)$ term is the stochastic variance floor. Accurate probe/dither tracking reduces the former, and anchor/control-variate updates reduce the latter.

Assumption 4 (PŁ inequality). There exists $\mu > 0$ such that $\frac{1}{2}\|\nabla \tilde{L}(W)\|^2 \geq \mu(\tilde{L}(W) - \tilde{L}^*)$ on the window.

Theorem 2 (PŁ regime). *Under Assumps. 1 to 4 and $\eta \leq 1/(2L_s)$,*

$$\mathbb{E}[\tilde{L}(W_t) - \tilde{L}^*] \leq (1 - \eta\mu)^t (\tilde{L}(W_0) - \tilde{L}^*) + O(\rho\sigma_{\text{vr}}^2\eta/\mu + \varepsilon^2/\mu).$$

Interpretation. In the PŁ regime, JacQuant inherits the same linear contraction as smooth stochastic optimization. The asymptotic neighborhood is smaller when B_t is closer to $J(W_t)$ and when the VR anchor lowers the variance. Spectral damping further helps in practice by suppressing large updates in saturated regions before they can create oscillations.

4.5 Composition Across Windows and Learner Convergence

The windowed analysis remains meaningful across training because code changes can be treated as a sequence of small perturbations to the local surrogate, provided the changes become milder as training stabilizes. Equivalently, a full QAT trajectory stitches together many local smooth problems; the drift term below measures the cost of moving from one local problem to the next.

Assumption 5 (Vanishing inter-window drift). For successive code-preserving windows k , the corresponding surrogates satisfy $\|\nabla \tilde{L}^{(k+1)}(W) - \nabla \tilde{L}^{(k)}(W)\| \leq \delta_k$ on visited iterates, with $\delta_k \downarrow 0$ and $\sum_k \delta_k < \infty$.

Theorem 3 (Global composition across windows). *If each window satisfies Thm. 1 or Thm. 2, then the same rates hold with an additional drift term $O(\delta_k^2)$ in the non-convex bound and $O(\delta_k/\mu)$ in the PŁ bound. If code assignments eventually stabilize, the PŁ trajectory is globally linearly convergent; if small flips persist with $\delta_k \rightarrow 0$, the convergence neighborhood shrinks accordingly.*

Assumption 6 (SA conditions for B). The B updates use Robbins–Monro stepsizes, persistent probe/dither excitation, compact projection for the chosen diagonal/block-diagonal class, a locally contractive mean-field operator, and slower drift of W_t .

Table 1: QAT results under symmetric uniform quantization.

(a) LLaMA3-1B, A16.							(b) LLaMA3-3B and Qwen3-1.7B, A8.							
Metrics	W1A16		W1.58A16		W2A16		LLaMA3-3B				Qwen3-1.7B			
	PPL	Acc.	PPL	Acc.	PPL	Acc.	W1A8		W1.58A8		W1A8		W2A8	
	PPL	Acc.	PPL	Acc.	PPL	Acc.	PPL	Acc.	PPL	Acc.	PPL	Acc.	PPL	Acc.
FP16 Baseline	9.6	58.5	9.6	58.5	9.6	58.5								
RTN (PTQ)	4.2e8	33.7	1.8e6	36.2	1.5e6	38.5								
GPTQ (PTQ)	3.3e8	32.7	4.6e4	32.8	3.3e2	36.8								
SpinQuant (PTQ)	2.4e8	33.7	2.2e3	32.6	46.7	38.3								
ParetoQ	17.9	51.9	14.8	54.3	13.5	55.7								
+Rotation Trick	18.1	52.0	14.2	54.7	13.3	56.1								
+JacQuant	17.6	52.4	13.9	55.3	12.3	56.6								
WinQ	15.3	52.6	12.9	55.6	11.9	56.6								
+JacQuant	15.1	53.5	12.3	56.1	11.8	56.8								

(c) LLaMA3-8B, W2A16.						
Metrics	30K		60K		90K	
	PPL	Acc.	PPL	Acc.	PPL	Acc.
ParetoQ	11.78	58.54	10.43	60.67	9.79	61.41
+JacQuant	11.69	59.10	10.32	60.98	9.71	62.04

Lemma 7 (Mean-field identification). *On a fixed window, both the probe and dither mean-field operators have $J_g(W)$ as the unique fixed point within the chosen group structure.*

Proposition 2 (Convergence and stability of the Jacobian learner). *Under Assumps. 1 and 6 and Lem. 7, $B_t^{(g)} \rightarrow J_g(W)$ almost surely on a fixed window, and under slow drift it tracks $J_g(W_t)$ with the contraction form in Prop. 1.*

Overall conclusion. The lemmas and theorems serve distinct roles. Lem. 1 identifies the bias that JacQuant must reduce; Lems. 2 and 3, Prop. 1, and Cor. 1 show that the learned map can reduce it; Lems. 4 and 5 guarantee stable surrogate gradients; and Thms. 1 to 3 and Prop. 2 show that these ingredients preserve standard convergence behavior while improving the constants most affected by low-bit saturation.

5 Experiments

We present a comprehensive empirical evaluation of JacQuant on modern LLMs under ultra-low-bit QAT. Our experiments are designed to (i) validate the central thesis that *learning a quantization Jacobian surrogate* improves optimization over the fixed STE surrogate, (ii) quantify end-task benefits on both perplexity and downstream reasoning accuracy, and (iii) demonstrate that the gains come at negligible memory/runtime cost. Throughout, JacQuant is a *drop-in backward-rule replacement*: the forward quantizer, model, data, and optimizer remain unchanged.

Experimental setup. We evaluate JacQuant on three representative LLM families (LLaMA3-1B/3B (Grattafiori et al., 2024) and Qwen3-1.7B (Yang et al., 2025)) under symmetric uniform QAT with per-channel scaling, focusing on ultra-low-bit regimes ($W \leq 2$, A8/A16). We also include a LLaMA3-8B W2A16 trajectory and a matched Rotation Trick (Fifty et al., 2025) comparison on LLaMA3-1B. We compare against popular QAT methods ParetoQ (Liu et al., 2025b) and WinQ (Li et al., 2026). All methods share identical model architectures, training data, optimization settings, and forward quantization, and differ only in their backward gradient rules. Scale/clipping handling is kept exactly the same as in the corresponding base QAT pipeline; JacQuant adds only the learned backward sensitivity map $B(W)$ and does not introduce a separate scale/clipping advantage. We report validation perplexity on WikiText-2 and zero-shot accuracy on eight standard benchmarks. Appendix F provides the detailed experimental settings and baseline definitions.

Main QAT results. Tab. 1a shows that replacing the identity-STE backward rule with JacQuant improves two strong QAT pipelines under the same forward quantizer. On LLaMA3-1B, ParetoQ +JacQuant improves PPL/Acc. from 17.9/51.9 to 17.6/52.4 at W1A16, from 14.8/54.3 to 13.9/55.3 at W1.58A16, and from 13.5/55.7 to 12.3/56.6 at W2A16. The matched Rotation Trick row gives a direct beyond-STE comparison: JacQuant is better at all three bit-widths, with the largest gap at W2A16 (13.3/56.1 \rightarrow 12.3/56.6). WinQ +JacQuant shows the same trend, reaching the best mean accuracy in the table (56.8). PTQ baselines degrade sharply at 1–2 bits, confirming that this is a genuinely difficult ultra-low-bit regime.

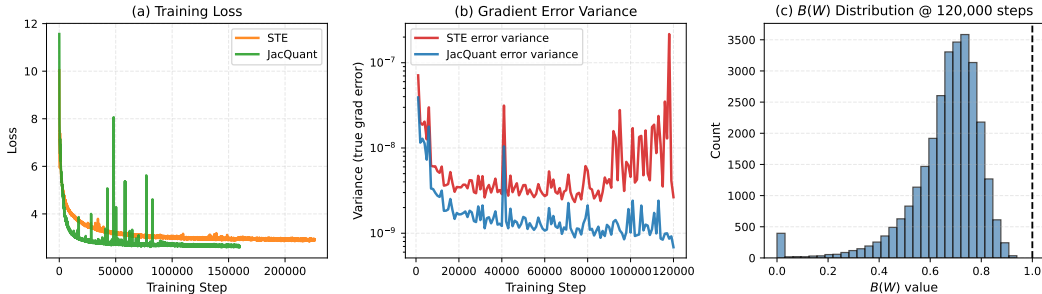


Figure 2: *Finite-difference gradient diagnostics*. (a) JacQuant converges faster than STE and stabilizes within a smaller neighborhood; (b) variance of the coordinate-wise mismatch between a central-difference reference gradient and the approximate training gradients; (c) histogram of the learned group-wise Jacobian scalars b_g at the target step, with the dashed line indicating the STE identity ($b = 1$).

Scaling to other families and the 8B run. Tab. 1b extends the matched-forward comparison to LLaMA3-3B and Qwen3-1.7B: JacQuant improves both PPL and mean accuracy at W1A8/W1.58A8 for LLaMA3-3B and at W1A8/W2A8 for Qwen3-1.7B. Tab. 1c adds the LLaMA3-8B W2A16 trajectory. Across 30K/60K/90K checkpoints, JacQuant monotonically improves ParetoQ from 11.78/58.54 to 11.69/59.10, from 10.43/60.67 to 10.32/60.98, and from 9.79/61.41 to 9.71/62.04 (PPL/Acc.). These gains are modest but consistent, suggesting that the learned backward sensitivity remains useful beyond the smaller matched-ablation suite.

Mechanistic diagnostic. Because hard quantizers are non-differentiable, we use finite differences only as a diagnostic reference: for sampled coordinates, we estimate $\hat{J}_i^{\text{FD}} = (Q_\Delta(w_i + \epsilon) - Q_\Delta(w_i - \epsilon))/(2\epsilon)$ and compare $\hat{J}_i^{\text{FD}}v_i$ with each training rule. Fig. 2 shows that JacQuant has lower coordinate-wise gradient-error variance than STE and learns group gains below one in locally insensitive/clipped regions. The small loss transients are expected because JacQuant periodically refreshes $B(W)$; they do not contradict the diagnostic or final metrics, which both favor the learned surrogate.

Efficiency and ablations. JacQuant stores one scalar sensitivity per quantization group (15–30MB in our LLM settings, $< 1.5\%$ of Adam-state memory) and refreshes it only every 50–200 steps. The runtime appendix (App. H) reports both the LLaMA3-1B W2A16 throughput suite and the LLaMA3-8B W2A16 step-time table. In the 1B suite, overhead is typically $\sim 1\text{--}5\%$ depending on group size and estimator; on LLaMA3-8B, practical Probe settings with $g_s \in \{32, 128\}$ stay within 0.8% of the STE baseline, and Dither remains within roughly 1.6%. Tab. 9 further shows a broad near-optimal region rather than fragile tuning: e.g., $g_s = 32/\text{uf}=200$ gives 12.3 PPL and 56.6 Avg. Acc., while $g_s = 128/\text{uf}=100$ or 200 remains close at 12.3–12.5 PPL and 56.3–56.5 Avg. Acc. This supports the design choice of amortized, moderately coarse sensitivity learning rather than aggressive per-step refresh.

6 Discussion and Future Work

The experiments substantiate the theoretical picture in Sec. 4: ultra-low-bit QAT is bottlenecked not only by the forward quantizer, but also by the backward model used to train through it. Across LLaMA3 and Qwen3 families, the LLaMA3-8B W2A16 trajectory, and the matched Rotation Trick comparison, JacQuant improves perplexity and zero-shot accuracy without changing the deployed hard quantizer. Mechanistically, the learned $B(W)$ acts as an adaptive gain controller: it stays near identity in responsive bin interiors and damps saturated/clipped directions where the mean-field sensitivity is smaller than one.

The practical claim is therefore deliberately scoped. JacQuant is a drop-in STE-free backward rule for ultra-low-bit LLM QAT, with end-to-end empirical evidence up to LLaMA3-8B and runtime measurements on both LLaMA3-1B W2A16 and LLaMA3-8B W2A16. Larger end-to-end QAT runs remain an empirical direction, but the current measurements indicate that the added state and throughput cost of learning $B(W)$ are small under practical group sizes. Limitations, non-uniform quantizer extensions, and additional ablations are discussed in App. A.

References

- Agustsson, E., Mentzer, F., Tschannen, M., Cavigelli, L., Timofte, R., Benini, L., and Gool, L. V. Soft-to-hard vector quantization for end-to-end learning compressible representations. *Advances in neural information processing systems*, 30, 2017.
- Bengio, Y., Léonard, N., and Courville, A. Estimating or propagating gradients through stochastic neurons for conditional computation. *arXiv preprint arXiv:1308.3432*, 2013.
- Bhalgat, Y., Lee, J., Nagel, M., Blankevoort, T., and Kwak, N. Lsq+: Improving low-bit quantization through learnable offsets and better initialization. In *Proceedings of the IEEE/CVF conference on computer vision and pattern recognition workshops*, pp. 696–697, 2020.
- Bisk, Y., Zellers, R., Gao, J., Choi, Y., et al. Piqa: Reasoning about physical commonsense in natural language. In *Proceedings of the AAAI Conference on Artificial Intelligence*, volume 34, pp. 7432–7439, 2020.
- Chee, J., Cai, Y., Kuleshov, V., and De Sa, C. M. Quip: 2-bit quantization of large language models with guarantees. *Advances in Neural Information Processing Systems*, 36:4396–4429, 2023.
- Choi, J., Wang, Z., Venkataramani, S., Chuang, P. I.-J., Srinivasan, V., and Gopalakrnan, K. Pact: Parameterized clipping activation for quantized neural networks. *arXiv preprint arXiv:1805.06085*, 2018. URL <https://arxiv.org/abs/1805.06085>.
- Clark, C., Lee, K., Chang, M.-W., Kwiatkowski, T., Collins, M., and Toutanova, K. Boolq: Exploring the surprising difficulty of natural yes/no questions. In *Proceedings of the 2019 Conference of the North American Chapter of the Association for Computational Linguistics: Human Language Technologies, Volume 1 (Long and Short Papers)*, pp. 2924–2936, 2019.
- Clark, P., Cowhey, I., Etzioni, O., Khot, T., Sabharwal, A., Schoenick, C., and Tafjord, O. Think you have solved question answering? try arc, the ai2 reasoning challenge. *arXiv preprint arXiv:1803.05457*, 2018.
- Cutkosky, A. and Orabona, F. Momentum-based variance reduction in non-convex sgd. *Advances in neural information processing systems*, 32, 2019.
- Defazio, A., Bach, F., and Lacoste-Julien, S. Saga: A fast incremental gradient method with support for non-strongly convex composite objectives. *Advances in neural information processing systems*, 27, 2014.
- Egiazarian, V., Panferov, A., Kuznedev, D., Frantar, E., Babenko, A., and Alistarh, D. Extreme compression of large language models via additive quantization. *arXiv preprint arXiv:2401.06118*, 2024.
- Esser, S. K., McKinstry, J. L., Bablani, D., Appuswamy, R., and Modha, D. S. Learned step size quantization. In *International Conference on Learning Representations*, 2020.
- Fang, C., Li, C. J., Lin, Z., and Zhang, T. Spider: Near-optimal non-convex optimization via stochastic path-integrated differential estimator. *Advances in neural information processing systems*, 31, 2018.
- Fifty, C., Junkins, R. G., Duan, D., Iyengar, A., Liu, J. W., Amid, E., Thrun, S., and Re, C. Restructuring vector quantization with the rotation trick. In *The Thirteenth International Conference on Learning Representations*, 2025.
- Frantar, E., Ashkboos, S., Hoefler, T., and Alistarh, D. Gptq: Accurate quantization for generative pre-trained transformers. In *The Eleventh International Conference on Learning Representations*, 2023.
- Gower, R. M., Richtárik, P., and Bach, F. Stochastic quasi-gradient methods: Variance reduction via jacobian sketching. *Mathematical Programming*, 188(1):135–192, 2021.
- Grattafiori, A., Dubey, A., Jauhri, A., Pandey, A., Kadian, A., Al-Dahle, A., Letman, A., Mathur, A., Schelten, A., Vaughan, A., et al. The llama 3 herd of models. *arXiv preprint arXiv:2407.21783*, 2024.

- Hofmann, T., Lucchi, A., Lacoste-Julien, S., and McWilliams, B. Variance reduced stochastic gradient descent with neighbors. *Advances in Neural Information Processing Systems*, 28, 2015.
- Jiang, W., Yang, S., Wang, Y., and Zhang, L. Adaptive variance reduction for stochastic optimization under weaker assumptions. *Advances in Neural Information Processing Systems*, 37:22047–22080, 2024.
- Johnson, R. and Zhang, T. Accelerating stochastic gradient descent using predictive variance reduction. *Advances in neural information processing systems*, 26, 2013.
- Karimi, H., Nutini, J., and Schmidt, M. Linear convergence of gradient and proximal-gradient methods under the polyak-łojasiewicz condition. In *Joint European conference on machine learning and knowledge discovery in databases*, pp. 795–811. Springer, 2016.
- Li, D., Liu, Z., Yi, K., Zhao, C., Krishnamoorthi, R., Khaitan, H., Zhang, H. R., and Li, S. Winq: Accelerating quantization-aware training of llms around saddle points. *ICML*, 2026.
- Li, Z., Hanzely, S., and Richtárik, P. Zerosarah: Efficient nonconvex finite-sum optimization with zero full gradient computation. *arXiv preprint arXiv:2103.01447*, 2021.
- Lin, J., Tang, J., Tang, H., Yang, S., Chen, W.-M., Wang, W.-C., Xiao, G., Dang, X., Gan, C., and Han, S. Awq: Activation-aware weight quantization for on-device llm compression and acceleration. *Proceedings of machine learning and systems*, 6:87–100, 2024.
- Liu, J., Su, J., Yao, X., Jiang, Z., Lai, G., Du, Y., Qin, Y., Xu, W., Lu, E., Yan, J., et al. Muon is scalable for llm training. *arXiv preprint arXiv:2502.16982*, 2025a.
- Liu, Y., Wen, J., Wang, Y., Ye, S., Zhang, L. L., Cao, T., Li, C., and Yang, M. Vptq: Extreme low-bit vector post-training quantization for large language models. In *Proceedings of the 2024 Conference on Empirical Methods in Natural Language Processing*, pp. 8181–8196, 2024.
- Liu, Z., Zhao, C., Huang, H., Chen, S., Zhang, J., Zhao, J., Roy, S., Jin, L., Xiong, Y., Shi, Y., Xiao, L., Tian, Y., Soran, B., Krishnamoorthi, R., Blankevoort, T., and Chandra, V. Paretoq: Improving scaling laws in extremely low-bit llm quantization. In *Advances in Neural Information Processing Systems*, 2025b.
- Malinovskii, V., Mazur, D., Ilin, I., Kuznedelev, D., Burlachenko, K., Yi, K., Alistarh, D., and Richtarik, P. Pv-tuning: Beyond straight-through estimation for extreme llm compression. *Advances in Neural Information Processing Systems*, 37:5074–5121, 2024.
- Malinovsky, G., Yi, K., and Richtárik, P. Variance reduced proxskip: Algorithm, theory and application to federated learning. *Advances in Neural Information Processing Systems*, 35:15176–15189, 2022.
- Merity, S., Xiong, C., Bradbury, J., and Socher, R. Pointer sentinel mixture models. In *International Conference on Learning Representations*, 2017.
- Mihaylov, T., Clark, P., Khot, T., and Sabharwal, A. Can a suit of armor conduct electricity? a new dataset for open book question answering. In *Proceedings of the 2018 Conference on Empirical Methods in Natural Language Processing*, pp. 2381–2391, 2018.
- Nagel, M., Amjad, R. A., Van Baalen, M., Louizos, C., and Blankevoort, T. Up or down? adaptive rounding for post-training quantization. In *International conference on machine learning*, pp. 7197–7206. PMLR, 2020.
- Nguyen, L. M., Liu, J., Scheinberg, K., and Takáč, M. Sarah: A novel method for machine learning problems using stochastic recursive gradient. In *International conference on machine learning*, pp. 2613–2621. PMLR, 2017.
- Penedo, G., Kydlíček, H., Lozhkov, A., Mitchell, M., Raffel, C. A., Von Werra, L., Wolf, T., et al. The fineweb datasets: Decanting the web for the finest text data at scale. *Advances in Neural Information Processing Systems*, 37:30811–30849, 2024.
- Roux, N. L., Schmidt, M., and Bach, F. A stochastic gradient method with an exponential convergence rate for finite training sets. *Advances in Neural Information Processing Systems*, 25, 2012.

- Sakaguchi, K., Bras, R. L., Bhagavatula, C., and Choi, Y. Winogrande: An adversarial winograd schema challenge at scale. In *Proceedings of the AAAI Conference on Artificial Intelligence*, volume 34, pp. 8732–8740, 2020.
- Sap, M., Rashkin, H., Chen, D., LeBras, R., and Choi, Y. Socialiqa: Commonsense reasoning about social interactions. In *Proceedings of the 2019 Conference on Empirical Methods in Natural Language Processing and the 9th International Joint Conference on Natural Language Processing (EMNLP-IJCNLP)*, pp. 4463–4473, 2019.
- Tan, Q., Song, X., Lu, J., Li, G., Liu, J., Hong, L., Ding, C., Li, J., Zhai, X., Huang, S., Niu, W., and Yuan, G. End-to-end on-device quantization-aware training for llms at inference cost. *arXiv preprint arXiv:2509.00031*, 2025.
- Tseng, A., Chee, J., Sun, Q., Kuleshov, V., and De Sa, C. Quip #: Even better llm quantization with hadamard incoherence and lattice codebooks. In *International Conference on Machine Learning*, pp. 48630–48656. PMLR, 2024.
- Xiao, G., Lin, J., Seznec, M., Wu, H., Demouth, J., and Han, S. Smoothquant: Accurate and efficient post-training quantization for large language models. In *International conference on machine learning*, pp. 38087–38099. PMLR, 2023.
- Yang, A., Li, A., Yang, B., Zhang, B., Hui, B., Zheng, B., Yu, B., Gao, C., Huang, C., Lv, C., et al. Qwen3 technical report. *arXiv preprint arXiv:2505.09388*, 2025.
- Yang, N. and Aamodt, T. M. Improving the straight-through estimator with zeroth-order information. *arXiv preprint arXiv:2510.23926*, 2025.
- Yao, Z., Yazdani Aminabadi, R., Zhang, M., Wu, X., Li, C., and He, Y. Zeroquant: Efficient and affordable post-training quantization for large-scale transformers. *Advances in neural information processing systems*, 35:27168–27183, 2022.
- Yao, Z., Wu, X., Li, C., Youn, S., and He, Y. Zeroquant-v2: Exploring post-training quantization in llms from comprehensive study to low rank compensation. *arXiv preprint arXiv:2303.08302*, 2023.
- Yin, P., Lyu, J., Zhang, S., Osher, S., Qi, Y., and Xin, J. Understanding straight-through estimator in training activation quantized neural nets. In *International Conference on Learning Representations*, 2019.
- Zellers, R., Holtzman, A., Bisk, Y., Farhadi, A., and Choi, Y. Hellaswag: Can a machine really finish your sentence? In *Proceedings of the 57th Annual Meeting of the Association for Computational Linguistics*, pp. 4791–4800, 2019.
- Zhou, S., Wu, Y., Ni, Z., Zhou, X., Wen, H., and Zou, Y. Dorefa-net: Training low bitwidth convolutional neural networks with low bitwidth gradients. *arXiv preprint arXiv:1606.06160*, 2016. URL <https://arxiv.org/abs/1606.06160>.

Contents

1	Introduction	1
2	Related Work	2
3	Method	3
3.1	Preliminaries: Grouped Quantization in LLMs	3
3.2	The Core Idea: Learning the Quantization Jacobian	3
3.3	Practical Estimation of $B(W)$	4
3.4	Optional Variance Reduction	4
4	Convergence Analysis of JacQuant	4
4.1	Local Smoothness and the Target Gradient	5
4.2	Why the Learned $B(W)$ Tracks $J(W)$	5
4.3	Stability of the Surrogate Gradient	6
4.4	Windowed and End-to-End Rates	6
4.5	Composition Across Windows and Learner Convergence	7
5	Experiments	8
6	Discussion and Future Work	9
A	Limitations and Future Work	15
B	Broader Impacts	15
C	Extended Related Work	15
C.1	LLM Quantization	15
C.2	Beyond the Straight-Through Estimator	16
C.3	Variance Reduction in Stochastic Optimization	17
D	Implementation Primitives for JacQuant-VR	18
E	Non-Variance-Reduced Variants of JacQuant	19
F	Detailed Experimental Setup and Baselines	21
F.1	Experimental Setup	21
G	Zero-Shot Generalization: Complementary Results	21
H	Runtime Overhead	23
I	Ablation Studies	24
I.1	Effect of Jacobian Group Size and Update Frequency	24

I.2	Probe vs. Dither Jacobian Learners	25
J	Missing Proofs	25
J.1	Proof of Lem. 2	25
J.2	Proof of Prop. 1	27
J.3	Proof of Lem. 3	28
J.4	Proof of Cor. 1	28
J.5	Proof of Thm. 1	28
J.6	Proof of Thm. 2	29
J.7	Proof of Theorem 3	30
J.8	Proof of Lem. 7	31
J.9	Proof of Prop. 2	32

A Limitations and Future Work

While JacQuant already improves stability and final quality in ≤ 2 -bit LLM QAT, several directions remain open. First, extending Jacobian learning to **mixed-precision policies** and more aggressive **activation quantization** (including dynamic-activation and heterogeneous regimes) would broaden applicability beyond the weight-centric configurations emphasized here; a natural approach is to learn coupled sensitivity surrogates for weights, activations, and clipping/scale parameters. Second, **broader scaling** remains an important empirical direction. The present paper includes an 8B W2A16 accuracy trajectory and explicit runtime measurements on both LLaMA3-1B W2A16 and LLaMA3-8B W2A16; still larger end-to-end QAT runs would further test how far the learned-backward-rule advantage persists. Third, there is room to improve the **estimation and scheduling** of $B(W)$: although Probe currently outperforms Dither in our implementation (Appendix I.1), refined dither statistics, adaptive probe scales, and refresh criteria tied to quantization drift could improve robustness under frequent code changes. Finally, on the theory side, sharpening **non-convex guarantees beyond PL** and relaxing reliance on code-preserving windows to better capture frequent bin flips in transformer training remains an important challenge; addressing it would deepen understanding of why and when learned sensitivity maps most effectively stabilize quantized optimization.

B Broader Impacts

This work studies a training algorithm for low-bit LLM quantization rather than a new model, dataset, or deployment product. Its main positive impact is efficiency: more stable ultra-low-bit QAT can reduce memory footprint and training/inference cost, which may lower energy use and make model compression research more accessible. The same efficiency gains may also make capable language models easier to deploy, including in applications with potential misuse or fairness, privacy, and safety concerns. JacQuant does not introduce new model capabilities or collect new data, so these risks primarily inherit from the underlying models and deployment contexts. Responsible use should therefore follow the licenses, safety policies, evaluation protocols, and monitoring practices associated with the base models and downstream applications.

C Extended Related Work

C.1 LLM Quantization

Post-Training Quantization (PTQ). PTQ avoids gradient updates by calibrating a pretrained model with a small dataset. For LLMs, SmoothQuant (Xiao et al., 2023) smooths activation outliers via an offline migration of scale from activations to weights, enabling accurate W8A8 deployment across many LLMs. GPTQ (Frantar et al., 2023) introduces a highly accurate, per-layer Hessian-informed weight quantizer that attains 3–4 bit weight-only compression with strong perplexity retention. ZeroQuant/ZeroQuant-V2 (Yao et al., 2022, 2023) propose affordable layer-by-layer PTQ pipelines with hardware-friendly kernels and calibration-friendly deployment. AWQ (Lin et al., 2024) further shows that protecting a small set of salient channels—identified by activations rather than weights—reduces quantization error and improves practical 4-bit inference. Overall, PTQ has become a strong default for training-free LLM deployment.

Quantization-Aware Training (QAT). Early QAT works established the use of the Straight-Through Estimator (STE) for backpropagating through non-differentiable quantizers. DoReFa-Net (Zhou et al., 2016) quantizes weights, activations, and gradients during training; PACT (Choi et al., 2018) learns activation clipping levels end-to-end; and LSQ/LSQ+ (Esser et al., 2020; Bhalgat et al., 2020) learn per-layer step sizes, narrowing the accuracy gap at low bitwidths. Despite empirical success, most QAT methods inherit STE’s bias, which ignores discrete bin geometry and can induce optimization mismatch at 2–4 bits. Recent STE-free directions include proximal surrogates (e.g., PV-Tuning (Malinovskii et al., 2024)) and geometric transforms (e.g., the Rotation Trick (Fifty et al., 2025)). Forward-only zeroth-order QAT methods such as ZeroQAT (Tan et al., 2025) attack a complementary scalability bottleneck by changing how gradients are estimated; JacQuant instead replaces only the backward map used with the deployed hard quantizer.

Why QAT for low-bit LLMs. Consistent with recent observations (e.g., ParetoQ (Liu et al., 2025b), WinQ (Li et al., 2026)), QAT typically outperforms PTQ under aggressive settings (≤ 2 -bit weights

and/or W&A quantization), because the optimizer can adapt layer scales and clipping behavior to the task distribution rather than relying solely on calibration statistics. Motivated by this, our work focuses on QAT but replaces the fixed STE with a *learned* surrogate Jacobian that adapts to local quantization geometry.

C.2 Beyond the Straight-Through Estimator

Most QAT methods still rely on the Straight-Through Estimator (STE) or its clipped variants to approximate the non-differentiable backward path (Esser et al., 2020; Bhalgat et al., 2020; Frantar et al., 2023; Chee et al., 2023; Tseng et al., 2024). Recent work explores several strategies to mitigate STE mismatch: (i) analytic/proximal backward surrogates (e.g., PV-Tuning (Malinovskii et al., 2024)), (ii) fixed geometric transforms (e.g., Rotation Trick (Fifty et al., 2025)), (iii) differentiable relaxations and continuation schedules (e.g., Soft-to-Hard VQ (Agustsson et al., 2017)), and (iv) hybrid first/zeroth-order estimators that use finite-difference probes to correct STE bias (e.g., FOGZO (Yang & Aamodt, 2025)). In parallel, extreme low-bit LLM methods may modify the optimizer geometry (e.g., Muon (Liu et al., 2025a)).

Why Jacobian learning? We target the core failure mode shared by these settings: the backward pass lacks a faithful local sensitivity model for the (piecewise-constant) quantizer. JacQuant therefore *keeps the hard quantizer in the forward pass* but learns a lightweight surrogate Jacobian $B(W)$ to approximate the quantizer’s mean-field sensitivity, reducing gradient bias exactly where STE is most problematic (near clipping/saturation) while remaining a drop-in replacement with negligible overhead.

JacQuant vs. PV-Tuning. PV-Tuning (Malinovskii et al., 2024) eliminates STE by reformulating quantization as a proximal optimization problem. Instead of copying gradients through the quantizer, it introduces an analytic surrogate via a proximal operator with explicit convergence guarantees. However, the resulting Jacobian is *static*: it depends on the proximal regularization and does not adapt to local loss curvature or quantization geometry. In contrast, JacQuant learns a *data-driven surrogate Jacobian* $B(W)$ that captures backward sensitivity through stochastic probing or dithering, dynamically aligning gradient propagation with the quantized landscape. As a result, JacQuant can adapt its backward gain across groups/layers and over time (e.g., damping saturated coordinates), improving stability and convergence in ultra-low-bit regimes without changing the forward quantizer.

JacQuant vs. Rotation Trick. The Rotation Trick (Fifty et al., 2025) mitigates STE bias via a fixed geometric constraint (preserving an angle relationship), but still uses a hand-crafted static transform. In contrast, JacQuant learns an adaptive surrogate Jacobian $B(W)$ that models how perturbations in weights affect quantized parameters, generalizing fixed rotations as a special case. This adaptivity is crucial when quantization sensitivity is heterogeneous across layers/groups, where a single fixed transform cannot simultaneously correct boundary effects and saturation behavior. The matched ParetoQ comparison in Tab. 1a makes this distinction quantitative: JacQuant improves over Rotation Trick at W1A16, W1.58A16, and W2A16, with the largest PPL gap at W2A16 (13.3→12.3).

JacQuant vs. Soft-to-Hard VQ. Soft-to-Hard VQ (Agustsson et al., 2017) optimizes a *smoothed* relaxation of quantization and gradually anneals toward hard assignments, enabling gradients to flow through the relaxed objective early in training. This is effective when a continuation schedule is acceptable and when the relaxed objective closely tracks the deployed hard quantizer. *Why we do not rely on relaxation*: for low-bit LLM QAT, the forward operator used at deployment is typically a fixed hard quantizer, and a soft relaxation can introduce a train–deploy mismatch that depends on the annealing schedule and temperature. *JacQuant’s benefit*: JacQuant keeps the *exact hard quantizer* in the forward pass and instead learns a local backward sensitivity $B(W)$, which directly corrects gradient bias near bin boundaries and clipping/saturation while preserving forward faithfulness. The methods are complementary: relaxation can serve as a warm start, while JacQuant improves the final hard-quantized optimization by learning the missing backward model.

JacQuant vs. FOGZO (zeroth-order information). FOGZO (Yang & Aamodt, 2025) improves upon STE by injecting zeroth-order (finite-difference) information, producing a hybrid estimator that can correct STE when the straight-through gradient is unreliable. *Why we do not use per-step zeroth-order correction*: finite-difference corrections typically require additional forward evaluations and must be repeated frequently to remain accurate as weights drift. *JacQuant’s benefit*: JacQuant amortizes sensitivity estimation by learning a reusable surrogate Jacobian $B(W)$ (diagonal or block-

diagonal) and updating it only occasionally (e.g., on refresh steps), while using $B(W)$ to modulate standard backprop gradients on all other steps. This yields a principled bias/variance improvement with minimal runtime overhead, rather than paying repeated zeroth-order query cost at every iteration.

JacQuant vs. ZeroQAT. ZeroQAT (Tan et al., 2025) targets a different operating point: it uses forward-only zeroth-order estimation to reduce backpropagation memory and time costs. JacQuant instead stays inside standard first-order QAT and changes only the quantizer backward rule. Thus, ZeroQAT is a systems/estimation alternative for reducing QAT cost, whereas JacQuant is a drop-in gradient-surrogate replacement that can in principle be combined with memory-saving QAT recipes.

JacQuant vs. Muon. Muon (Liu et al., 2025a) is an optimizer that improves the *update geometry* for matrix parameters (e.g., orthogonalizing momentum) and can speed up or stabilize large-scale training in full precision. *Why we address the quantizer Jacobian:* optimizer improvements do not resolve the fact that the gradient signal itself is biased when backpropagating through a hard quantizer with STE. *JacQuant’s benefit:* JacQuant corrects the *gradient estimator* by learning the missing backward sensitivity map $B(W)$, and is therefore compatible with (and potentially enhanced by) better optimizers such as Muon. This separation of concerns lets us retain standard QAT pipelines and forward quantizers while directly targeting the STE-induced mismatch.

Applicability beyond uniform scalar quantizers. Our experiments focus on symmetric uniform LLM QAT because it is the cleanest setting for isolating the backward-rule contribution. The mechanism is nevertheless not tied to uniform bins: for separable non-uniform scalar quantizers, the same group-wise slope estimator can learn local sensitivities around non-equally-spaced thresholds; for vector, trellis, or codebook quantizers, the natural extension is to replace scalar group gains with richer block-structured $B(W)$ matching the quantizer block/codeword structure. These variants may require different probe covariance, block size, and refresh schedules, so we treat them as promising extensions rather than claims established by the present experiments.

These comparisons align with our analysis: JacQuant explicitly learns $B(W) \approx J(W)$, reducing bias to a principled target gradient and naturally damping saturated directions, whereas many alternatives either keep a static surrogate, change the forward objective, or pay repeated zeroth-order query cost.

C.3 Variance Reduction in Stochastic Optimization

Variance-reduced (VR) methods accelerate stochastic optimization by reducing gradient noise via control variates, including SAG (Roux et al., 2012), SVRG (Johnson & Zhang, 2013; Malinovsky et al., 2022), and SAGA (Defazio et al., 2014), with extensions such as SARAH (Nguyen et al., 2017; Li et al., 2021), SPIDER (Fang et al., 2018), and STORM (Cutkosky & Orabona, 2019; Jiang et al., 2024). Most of these works assume a (possibly noisy) *fixed* gradient oracle for a smooth objective and focus on shrinking the variance of minibatch gradients while preserving convergence rates. A practical distinction is that some classical VR schemes (notably SAG/SAGA) rely on *per-example memory* (control variates stored for all data indices), which becomes impractical for LLM-scale corpora and streaming training where the effective dataset size is massive.

Why VR is nontrivial for STE-free QAT. In JacQuant, stochasticity arises not only from minibatch sampling, but also from *learning the backward model itself*: we optimize using per-sample surrogate gradients $F_i(W) := B(W) v_i$ where $v_i = \nabla_q \ell(f(x_i; q), y_i)$ and $q = Q_\Delta(W)$, while $B(W)$ is estimated by stochastic probing/dithering and updated intermittently. This introduces an additional source of noise and drift beyond standard SGD/Adam, and naive frequent Jacobian updates can inject high-frequency variance that destabilizes training near quantization boundaries.

JacSketch connection and our adaptation (scalable VR for LLMs). JacSketch (Gower et al., 2021) interprets VR as *Jacobian sketching* for stochastic oracles, yielding low-variance quasi-gradient updates. A common and effective instantiation of this principle is SAGA-style memory (maintaining a table of historical per-index control variates), but such *dataset-sized* memory is typically infeasible for LLM training. JacQuant adopts the control-variate principle but is designed for the LLM regime: we (i) do *not* sketch the Jacobian of the loss; (ii) instead maintain a lightweight diagonal/block-diagonal surrogate of the *quantizer sensitivity* via $B(W)$; and (iii) use a *low-memory* VR estimator. In particular, our theory is VR-agnostic: we analyze a general class of variance-reduced estimators via an *ABC-type* oracle assumption (cf. the ABC bounds used in our convergence analysis), which covers a broad family of control-variate and anchor-based methods. Motivated by implementability at LLM

scale, we instantiate this framework with a lightweight L-SVRG (loopless SVRG)-style estimator that requires no per-example table.

Concretely, letting $F_S(W, B) := \frac{1}{|S|} \sum_{i \in S} F_i(W)$, the L-SVRG update takes the form

$$g_t = F_{S_t}(W_t, B_t) - F_{S_t}(\tilde{W}, \tilde{B}) + \tilde{g}, \quad \tilde{g} = \text{RefGrad}(\tilde{W}, \tilde{B}),$$

where $(\tilde{W}, \tilde{B}, \tilde{g})$ is an anchor state computed on a (full or large) reference batch and refreshed probabilistically. This reduces variance of the JacQuant *surrogate gradient* without changing the forward quantizer, while avoiding the $\mathcal{O}(n)$ memory footprint of SAGA/JacSketch tables.

Our key design: amortized refresh enables cheap and stable Jacobian learning. Inspired by skip/refresh VR frameworks (e.g., VR-ProxSkip (Malinovsky et al., 2022)), JacQuant refreshes the anchor state $(\tilde{W}, \tilde{B}, \tilde{g})$ only occasionally (e.g., with probability p or via a drift/variance criterion). Importantly, we also update $B(W)$ primarily on these refresh steps. This coupling is central in JacQuant: it (i) amortizes the cost of probing/dithering so most iterations remain as cheap as standard QAT, (ii) prevents noisy Jacobian estimates from dominating the optimization, and (iii) keeps the VR machinery *LLM-friendly* by using L-SVRG (constant-memory anchor state) rather than dataset-sized SAGA memory.

What is gained relative to “VR alone”. Variance reduction by itself only shrinks stochastic noise; it does not address the STE-induced *bias* caused by using an incorrect backward Jacobian. JacQuant separates these effects: Jacobian learning reduces bias by driving $B(W)$ toward the mean-field sensitivity, while VR tightens the remaining variance constant of stochastic updates. This combination yields a geometry-aware VR paradigm tailored to quantized optimization: forward quantization remains unchanged, while the backward path is both *bias-corrected* (via $B(W)$) and *variance-controlled* (via scalable VR).

D Implementation Primitives for JacQuant-VR

This appendix specifies the minimal “API” used by Alg. 1. Let $S \subset \{1, \dots, n\}$ be a minibatch, $q = Q_\Delta(W)$ (or $q = Q_\Delta(W+r) - r$ for DITHER), $v_i = \nabla_q \ell(f(x_i; q), y_i)$, and $F_i(W) = B(W) v_i$.

GradEst: General control-variate gradient estimator.

$$g = \underbrace{\frac{1}{|S|} \sum_{i \in S} (F_i(W) - h_i(s))}_{\text{stochastic difference}} + \underbrace{\tilde{g}}_{\text{reference term}},$$

where s is the VR state (e.g., a table), $h_i(s)$ the per-index control variate, and \tilde{g} is a reference gradient at anchor (\tilde{W}, \tilde{B}) .

Typical instantiations (choose one):

SVRG-like: $h_i(s) = F_i(\tilde{W}), \quad \tilde{g} = \text{RefGrad}(\tilde{W}, \tilde{B}) = \frac{1}{n} \sum_{j=1}^n F_j(\tilde{W}).$

SAGA-like: $s = \{Y_1, \dots, Y_n, \bar{Y} = \frac{1}{n} \sum_j Y_j\}, \quad h_i(s) = Y_i, \quad \tilde{g} = \bar{Y}.$

SARAH-like: refresh: $\tilde{g} = \frac{1}{|S_{\text{ref}}|} \sum_{j \in S_{\text{ref}}} F_j(W), \quad g = \tilde{g};$ else: $g = \frac{1}{|S|} \sum_{i \in S} (F_i(W) - F_i(W^-)) + g^-.$

RefGrad: Anchor/reference gradient.

$$\text{RefGrad}(\tilde{W}, \tilde{B}) = \frac{1}{|S_{\text{ref}}|} \sum_{i \in S_{\text{ref}}} \tilde{B} \nabla_q \ell(f(x_i; \tilde{q}), y_i), \quad \tilde{q} = Q_\Delta(\tilde{W}) \text{ (or } Q_\Delta(\tilde{W}+r) - r).$$

CtrlUpdate: Update of the VR state s .

$$\text{CtrlUpdate}(s, W, \tilde{W}; S) : \begin{cases} \text{SAGA-like: } Y_i \leftarrow F_i(W) \forall i \in S, \quad \bar{Y} \leftarrow \bar{Y} + \frac{1}{n} \sum_{i \in S} (F_i(W) - Y_i^{\text{old}}); \\ \text{SVRG-like: stateless; refresh sets } (\tilde{W}, \tilde{B}, \tilde{g}); \\ \text{SARAH-like: maintain recursive } g \text{ and previous } (W^-, g^-). \end{cases}$$

Algorithm 2 API reference for JacQuant-VR

```

1: function GRADEST( $W, B, \tilde{W}, \tilde{B}, \tilde{g}, s; S$ )
2:   return  $\frac{1}{|S|} \sum_{i \in S} (B \nabla_q \ell(f(x_i; q), y_i) - h_i(s)) + \tilde{g}$ 
3: end function
4: function REFGRAD( $\tilde{W}, \tilde{B}$ )
5:   Sample  $S_{\text{ref}}$  (full or large minibatch)
6:   return  $\frac{1}{|S_{\text{ref}}|} \sum_{i \in S_{\text{ref}}} \tilde{B} \nabla_q \ell(f(x_i; \tilde{q}), y_i)$ 
7: end function
8: function PROBEUPDATE( $W$ )
9:   for each group  $g$  do
10:    Draw  $\delta_g \sim \mathcal{N}(0, \sigma^2 I)$ ;  $\Delta q_g \leftarrow Q_\Delta(W_g + \delta_g) - Q_\Delta(W_g)$ 
11:     $\hat{B}_g \leftarrow \arg \min_{B \in \mathcal{B}_g} \|\Delta q_g - B \delta_g\|^2$  (diag/blk-diag LS)
12:     $B_g \leftarrow (1 - \beta) B_g + \beta \hat{B}_g$ 
13:   end for
14:   return  $B$ 
15: end function

```

ProbeUpdate: Probe-based Jacobian update. For each quantization group g (size d_g), draw $\delta_g \sim \mathcal{N}(0, \sigma^2 I)$, measure $\Delta q_g = Q_\Delta(W_g + \delta_g) - Q_\Delta(W_g)$, and apply an EMA least-squares step:

$$\hat{B}_g = \arg \min_{B \in \mathcal{B}_g} \|\Delta q_g - B \delta_g\|^2, \quad B_g \leftarrow (1 - \beta) B_g + \beta \hat{B}_g, \quad \mathcal{B}_g = \{\text{diag/block-diag}\}.$$

Diagonal one-step: $[\hat{B}_g]_{jj} = \frac{(\Delta q_g)_j \delta_{g,j}}{\delta_{g,j}^2 + \epsilon}$.

DitherEMA: Dither-based Jacobian update. With $r \sim \text{Unif}[-\frac{\Delta}{2}, \frac{\Delta}{2}]$, set $q = Q_\Delta(W + r) - r$ and update

$$B \leftarrow (1 - \beta) B + \beta \phi(W; r),$$

where $\phi(\cdot)$ is a diagonal/block-diagonal sensitivity statistic of (q, W) (damped near saturation).

E Non-Variance-Reduced Variants of JacQuant

This appendix provides additional implementation details of the proposed Jacobian-learning framework, including the full pseudocode for the non-variance-reduced (Base) variants (the main variance-reduced variant is provided in [Alg. 1](#)), as well as a summary table comparing their key characteristics.

JacQuant-VR (Main Algorithm). [Alg. 1](#) presents the unified variance-reduced version of JacQuant, which integrates the stochastic control-variate principle of JacSketch/SAGA into quantization-aware training. The algorithm maintains a table of historical Jacobian-modulated gradients $\{Y_i\}$ to construct a low-variance estimator:

$$g_t = \bar{Y} + \frac{1}{|S_t|} \sum_{i \in S_t} (F_i(W_t) - Y_i),$$

where \bar{Y} denotes the running mean. This estimator asymptotically matches the unbiased gradient of the surrogate loss but with reduced stochastic noise. The Jacobian $B(W)$ is learned either via PROBE (periodic perturbations) or DITHER (continuous randomization). This VR variant is the one used in all main-text experiments and theoretical results in [Sec. 4](#).

JacQuant-Base (Non-VR Variant). For completeness, [Alg. 3](#) provides the simpler non-variance-reduced version used for ablation studies. This baseline removes the JacSketch control-variate mechanism and uses the plain stochastic gradient

$$g_t = \frac{1}{|S_t|} \sum_{i \in S_t} F_i(W_t),$$

while keeping the same learned Jacobian updates (PROBE or DITHER). Although it has higher variance, this variant more directly reflects standard STE-style QAT pipelines and is computationally lighter. Empirically, it converges more slowly and exhibits larger oscillations near quantization boundaries—consistent with the variance-reduction analysis in [Sec. 4.4](#) and [Thm. 1](#).

Algorithm 3 JacQuant-Base (Non-Variance-Reduced): Unified Jacobian Learning for Uniform QAT (Appendix)

Require: Pretrained W , dataset \mathcal{D} , quantizer Q_Δ , step size η , batch size b , EMA $\beta \in (0, 1)$;

Require: mode $\in \{ \text{PROBE}, \text{DITHER} \}$; (Probe) probe scale σ , interval T_{probe}

- 1: Initialize $B \leftarrow I$ (diagonal or per-group)
- 2: **for** $t = 1, 2, \dots$ **do**
- 3: Sample minibatch $S_t \subset \mathcal{D}$
- 4: **if** mode = DITHER **then**
- 5: Draw $r \sim \mathcal{U}[-\frac{\Delta}{2}, \frac{\Delta}{2}]$, set $q \leftarrow Q_\Delta(W + r) - r$ ▷ Unbiased in mean
- 6: **else** ▷ Probe
- 7: $q \leftarrow Q_\Delta(W)$
- 8: **end if**
- 9: *// Per-sample grads and learned-Jacobian backprop*
- 10: **for** $i \in S_t$ **do**
- 11: $v_i \leftarrow \nabla_q \ell(f(x_i; q), y_i)$
- 12: **end for**
- 13: $g_t \leftarrow \frac{1}{|S_t|} \sum_{i \in S_t} B(W) v_i$
- 14: *// Any first-order optimizer (SGD/AdamW)*
- 15: $W \leftarrow W - \eta g_t$
- 16: **if** mode = PROBE **and** $t \bmod T_{\text{probe}} = 0$ **then**
- 17: **for** each group g **do**
- 18: Draw $\delta_g \sim \mathcal{N}(0, \sigma^2 I)$, $W_g^+ \leftarrow W_g + \delta_g$
- 19: $\Delta q_g \leftarrow Q_\Delta(W_g^+) - Q_\Delta(W_g)$
- 20: $B_g \leftarrow (1 - \beta)B_g + \beta \text{diag}\left(\frac{\Delta q_g \odot \delta_g}{\delta_g \odot \delta_g + \epsilon}\right)$ ▷ Probe-based B update
- 21: **end for**
- 22: **else if** mode = DITHER **then**
- 23: **for** each group g **do**
- 24: $B_g \leftarrow (1 - \beta)B_g + \beta \phi_g(W, r)$ ▷ EMA to I in interiors; damp near clipping
- 25: **end for**
- 26: **end if**
- 27: **end for**

Table 2: Comparison between JacQuant-VR and JacQuant-Base. VR integrates variance-reduced control variates (SAGA, SVRG, SARAH), while Base uses direct stochastic gradients. Both support Probe- and Dither-based Jacobian updates.

Feature	JacQuant-VR (Main)	JacQuant-Base (Ablation)
Gradient estimator	Control-variate (JacSketch)	Plain stochastic gradient
Variance level	Low ($\sim \rho \sigma^2$, $\rho < 1$)	High (σ^2)
Memory overhead	$\approx 1.5\%$ (gradient table)	Negligible
Convergence rate	$\mathcal{O}(1/T)$ / linear under PL	Same asymptotic, larger constants
Stability near clipping	Strong (damped $B(W)$ + low variance)	Moderate (no variance damping)
Recommended use	Main experiments, high precision	Ablations, small models

Comparison. Tab. 2 contrasts the two implementations. JacQuant-VR achieves lower variance and smoother training dynamics at the cost of a modest memory overhead for storing historical gradient tables (about 1.5% of Adam states). JacQuant-Base is stateless and slightly faster per step, but less stable in ultra-low-bit regimes (e.g., W2A16). Both share the same theoretical convergence guarantees when $B(W) \rightarrow J(W)$, but differ in variance constants.

Overall, the variance-reduced version is recommended for high-precision or large-scale training, while the base variant serves as a minimal, easy-to-integrate alternative.

F Detailed Experimental Setup and Baselines

F.1 Experimental Setup

Models and data. We evaluate on three representative LLM architectures: LLaMA3-1B, LLaMA3-3B (Grattafiori et al., 2024), and Qwen3-1.7B (Yang et al., 2025). We also report a LLaMA3-8B W2A16 trajectory to probe scaling behavior beyond the 1–3B matched-ablation suite. All models are trained on FineWebEdu (Penedo et al., 2024) for pre-training QAT and evaluated on WikiText-2 (Merity et al., 2017) for perplexity, plus eight standard zero-shot benchmarks including ARC-easy/challenge (Clark et al., 2018), BoolQ (Clark et al., 2019), PIQA (Bisk et al., 2020), SIQA (Sap et al., 2019), HellaSwag (Zellers et al., 2019), OBQA (Mihaylov et al., 2018), and WinoGrande (Sakaguchi et al., 2020).

Quantization configuration. We apply symmetric uniform quantization with per-channel scaling to all linear layers (attention Q/K/V projections, MLP up/down projections, output head). Bit-widths range from 1 to 2 bits for weights ($W_1, W_1.58, W_2$) and 8 to 16 bits for activations (A_8, A_{16}). We focus primarily on ultra-low-bit regimes ($W \leq 2$) where STE-based methods struggle most. Each quantization group contains 32–256 parameters; we use 128 as the default.

Training Details. All methods use identical forward quantization $Q(\cdot)$; only the *backward gradient rule* differs. We train with AdamW ($\beta_1 = 0.9, \beta_2 = 0.999, \varepsilon = 10^{-8}$), learning rate $\eta = 2 \times 10^{-5}$, constant schedule with 1k warmup steps, weight decay 0, batch size 8 per device, and gradient accumulation 1. Training runs for 240k steps with evaluation every 5k steps. For LLaMA3-8B, we report intermediate checkpoints at 30K/60K/90K due to the substantially higher end-to-end QAT cost. For JacQuant, we update the surrogate Jacobian $B(W)$ every 100 steps using EMA with $\beta = 0.9$ by default.

We perform a systematic grid search to determine the optimal hyperparameters for JacQuant. The search spans both the probe-based (JacQuant-Probe) and dither-based (JacQuant-Dither) variants, exploring probe noise levels $\sigma \in \{10^{-4}, 10^{-3}, 10^{-2}\}$, EMA coefficients $\beta \in \{0.8, 0.9, 0.95\}$, update frequencies $f_{\text{update}} \in \{50, 100, 200\}$, and group sizes $G \in \{32, 64, 128, 256\}$. We also evaluate the impact of optional JacSketch control variates for variance reduction. The final results are reported using the best-performing hyperparameter settings selected by validation perplexity on the WikiText-2 dataset. This grid is a development-time sweep rather than an added deployment requirement; after selecting defaults, the sensitivity study in Tab. 9 shows that performance varies mildly over a broad range of group sizes and refresh intervals.

Computational Overhead. The additional memory cost of JacQuant for storing $B(W)$ is $\mathcal{O}(G) \approx 15\text{--}30$ MB for typical LLMs, which is less than 1.5% of Adam optimizer states. Jacobian updates add negligible runtime overhead ($< 2\%$) since they occur infrequently (every 50–200 steps). The runtime study in Tabs. 7 and 8 reports measured overhead explicitly for both LLaMA3-1B W2A16 and LLaMA3-8B W2A16. For comparison, true gradient computation via finite differences (used only for validation) adds 10–20% overhead but is not needed during standard training.

Baselines We compare against representative QAT baselines: (i) STE (Bengio et al., 2013), the standard straight-through estimator with identity Jacobian; (ii) ParetoQ (Liu et al., 2025b) and WinQ (Li et al., 2026), which optimize Pareto-balanced or noise-regularized quantization under the same STE assumption; and (iii) our proposed JacQuant-Probe and JacQuant-Dither, which learn surrogate Jacobians via probing and dithering (Alg. 1).

Unless explicitly marked as JacQuant-BASE in Sec. E, all reported JacQuant results use the variance-reduced implementation; the base/non-VR variant is included only to isolate the effect of variance reduction. All baselines use identical model architectures, training data, optimization settings, and quantization configurations. All experiments are implemented in PyTorch 2.3 with custom CUDA kernels for quantization on 8 NVIDIA A100 (80GB) GPUs.

G Zero-Shot Generalization: Complementary Results

Tab. 1a-1c reports the mean zero-shot generalization performance over eight standard QA reasoning tasks. We provide the full set of complementary results for LLaMA3-1B (Tab. 3), LLaMA3-3B (Tab. 4), Qwen-1.7B (Tab. 5) and LLaMA3-8B (Tab. 6).

Table 3: **Zero-shot accuracy (%) on downstream reasoning tasks. LLaMA3-1B.** Models are trained with QAT on FineWebEdu and directly evaluated on reasoning benchmarks without fine-tuning. Higher is better. Best per column in **bold**.

Method	Wiki2 (\downarrow)	ARC-e	ARC-c	BoolQ	PIQA	SIQA	HellaS.	OBQA	Wino.	Avg. Acc. (\uparrow)
FP16 Baseline	9.6	64.8	42.5	64.8	74.8	44.8	64.4	50.2	61.5	58.5
LLaMA3-1B, W1A16										
RTN	4.2e8	25.0	22.5	37.6	49.5	32.9	25.0	27.1	49.6	33.7
GPTQ	3.3e8	26.9	21.7	37.6	51.8	33.5	25.5	14.8	49.7	32.7
SpinQuant	2.4e8	25.0	22.5	37.6	49.5	32.9	25.0	27.1	49.6	33.7
ParetoQ	17.9	58.7	39.8	62.6	67.4	42.4	46.9	43.9	53.5	51.9
+JacQuant	17.6	60.6	38.9	64.1	67.2	42.6	47.8	44.1	53.9	52.4
WinQ	15.3	59.7	37.0	61.3	69.5	42.6	49.8	46.1	54.4	52.6
+JacQuant	15.1	61.1	37.9	63.1	70.2	43.2	50.9	44.9	56.3	53.5
LLaMA3-1B, W1.58A16										
RTN	1.8e6	24.5	22.3	62.4	52.7	33.4	25.4	18.4	50.2	36.2
GPTQ	7.5e4	24.8	22.2	38.0	52.2	32.5	25.4	17.0	49.4	32.7
SpinQuant	5.8e3	25.3	22.5	37.6	51.6	33.3	25.3	17.6	48.5	32.7
ParetoQ	14.8	61.4	39.7	63.1	71.0	42.6	53.1	47.5	55.7	54.3
+JacQuant	13.9	64.2	38.2	62.2	71.6	44.4	55.0	47.7	59.1	55.3
WinQ	12.9	65.0	39.7	62.1	72.9	44.3	56.2	47.1	57.4	55.6
+JacQuant	12.3	66.1	39.2	63.4	73.6	44.8	56.9	47.5	57.1	56.1
LLaMA3-1B, W2A16										
RTN	1.5e6	24.5	23.1	62.4	52.3	33.6	25.4	17.6	50.3	36.2
GPTQ	3.8e4	26.9	21.7	37.6	51.8	33.5	25.5	14.8	49.7	32.7
SpinQuant	3.8e2	31.0	20.1	45.5	54.6	33.8	26.7	16.2	50.9	34.9
ParetoQ	13.5	63.1	41.9	62.5	72.8	43.6	55.2	49.2	57.3	55.7
+JacQuant	12.3	66.1	42.0	62.1	72.8	43.3	57.4	49.8	59.1	56.6
WinQ	11.9	65.0	42.5	62.5	73.8	43.2	58.4	48.1	59.1	56.6
+JacQuant	11.8	66.4	39.8	64.7	73.3	43.8	59.2	47.8	59.4	56.8

Table 4: **Zero-shot accuracy (%) on downstream reasoning tasks. LLaMA3-3B.** Models are trained with QAT on FineWebEdu and directly evaluated on reasoning benchmarks without fine-tuning. Higher is better. Best per column in **bold**.

Method	Wiki2 (\downarrow)	ARC-e	ARC-c	BoolQ	PIQA	SIQA	HellaS.	OBQA	Wino.	Avg. Acc. (\uparrow)
FP16 Baseline	7.7	72.6	50.7	74.6	78.2	48.5	74.3	53.7	69.2	65.2
LLaMA3-3B, W1A8										
RTN	7.3e7	25.0	22.5	37.6	49.5	32.9	25.0	27.1	49.6	33.7
GPTQ	5.9e7	26.6	21.9	37.6	52.5	33.7	25.6	15.0	49.4	32.8
SpinQuant	4.5e7	27.0	22.0	37.6	52.0	33.4	25.5	14.5	50.2	32.8
ParetoQ	15.7	63.1	39.1	63.0	70.9	42.6	50.6	46.7	56.5	54.1
+JacQuant	15.2	64.3	38.9	60.6	72.2	43.2	50.7	49.8	59.1	54.9
LLaMA3-3B, W1.58A8										
RTN	7.9e5	24.7	23.4	37.6	52.9	33.8	25.5	17.4	50.3	33.2
GPTQ	2.7e5	25.3	22.9	37.6	53.7	34.4	25.3	15.6	49.5	33.0
SpinQuant	3.1e3	26.6	23.4	39.1	52.7	34.7	25.3	16.4	48.5	33.3
ParetoQ	13.1	67.9	42.0	53.9	72.0	43.9	58.2	49.6	60.2	56.0
+JacQuant	12.7	67.3	42.0	57.5	73.4	43.8	59.1	51.8	61.3	57.1

Table 5: **Zero-shot accuracy (%) on downstream reasoning tasks.** Qwen-1.7B. Models are trained with QAT on FineWebEdu and directly evaluated on reasoning benchmarks without fine-tuning. Higher is better. Best per column in **bold**.

Method	Wiki2 (\downarrow)	ARC-e	ARC-c	BoolQ	PIQA	SIQA	HellaS.	OBQA	Wino.	Avg. Acc. (\uparrow)
FP16 Baseline	16.2	68.9	41.0	78.9	71.7	45.1	59.6	38.5	61.6	58.2
Qwen-1.7B, W1A8										
ParetoQ	46.5	42.0	26.2	61.4	59.8	40.0	29.1	28.9	50.8	42.3
+JacQuant	45.3	42.5	26.5	61.8	59.6	40.6	29.5	29.4	51.7	42.7
Qwen-1.7B, W2A8										
ParetoQ	22.2	52.9	32.6	62.4	65.1	42.7	41.2	32.8	53.1	47.9
+JacQuant	21.5	54.1	31.1	64.4	64.1	43.5	40.3	34.1	52.8	48.1

Table 6: **Zero-shot accuracy (%) on downstream reasoning tasks.** LLaMA3-8B with W2A16. Models are trained with QAT on FineWebEdu and directly evaluated on reasoning benchmarks without fine-tuning. Higher is better. Best per column in **bold**.

Method	Wiki2 (\downarrow)	ARC-e	ARC-c	BoolQ	PIQA	SIQA	HellaS.	OBQA	Wino.	Avg. Acc. (\uparrow)
30K										
ParetoQ	11.78	70.79	42.54	67.37	74.80	45.41	66.12	37.89	63.39	58.54
+JacQuant	11.69	69.65	44.95	67.55	74.88	44.86	66.65	39.94	64.32	59.10
60K										
ParetoQ	10.43	72.50	46.58	69.30	75.56	46.88	69.09	40.72	64.70	60.67
+JacQuant	10.32	72.74	46.21	70.73	75.42	46.92	68.91	41.12	65.80	60.98
90K										
ParetoQ	9.79	75.60	48.36	66.91	76.79	47.13	69.36	40.03	67.07	61.41
+JacQuant	9.71	75.48	49.42	70.31	76.93	47.53	69.44	41.31	65.88	62.04

H Runtime Overhead

A key practical goal of JacQuant is to improve low-bit QAT stability *without* sacrificing training throughput. Table 7 reports end-to-end training throughput (steps/second) for LLaMA3-1B W2A16 when augmenting two strong QAT baselines (ParetoQ and WinQ) with our Jacobian-learning back-propagation (JacQuant-Probe/ JacQuant-Dither).

Group size vs. throughput. We vary the Jacobian *group size* g_s , i.e., the number of weight elements that share a single scale/Jacobian entry in the block-diagonal surrogate $B(W)$. Larger g_s reduces the number of groups and thus decreases both (i) the memory traffic for reading/writing $B(W)$ and (ii) the amount of work in groupwise Jacobian updates (ProbeUpdate/DitherEMA), so it is expected to yield *higher* steps/second. This trend is visible in several settings; e.g., for WinQ with JacQuant-Probe, throughput increases from 1.7223 ($g_s = 8$) to 1.7392 ($g_s = 32$) to 1.7447 ($g_s = 128$). Despite the above expectation, the measured throughput is not strictly monotonic in all cases. For example, under WinQ +JacQuant-Dither, $g_s=32$ yields 1.7411 steps/s while $g_s=128$ yields 1.7308 steps/s. This difference is small (about 0.6%) and is well within typical run-to-run and measurement variability for large-scale training, where throughput can be affected by CUDA kernel scheduling, cache effects, data-loader jitter, and asynchronous execution/overlap. Crucially, the Jacobian-learning component is only a *small* fraction of the total transformer forward/backward cost, so these secondary system effects can mask the otherwise expected scaling with g_s when differences are at the sub-1% level.

Minimal overhead in practice. Across both baselines and both Jacobian estimators, JacQuant maintains throughput close to STE training. Relative to the STE baseline, the slowdown ranges from roughly 1–5% in this LLaMA3-1B W2A16 setting, while delivering the accuracy/stability benefits reported elsewhere. In particular, with the recommended larger group sizes (e.g., $g_s=128$), the overhead is consistently small (about 1.6% for WinQ +JacQuant-Probe and 3.5% for ParetoQ

+JacQuant-Probe), confirming that JacQuant is a practical drop-in replacement: the forward quantizer is unchanged, and the additional cost of learning/applying $B(W)$ is amortized by its lightweight block structure and infrequent updates.

Table 7: **Training throughput** (steps/s; higher is better) for LLaMA3-1B W2A16 QAT. g_s is the number of weights that share one scale / one (block-)Jacobian entry. Parentheses report relative throughput change vs. STE.

Base	STE	JacQuant-Probe (g_s)			JacQuant-Dither (g_s)		
		8	32	128	8	32	128
ParetoQ Liu et al. (2025b)	1.8074	1.7391 (-3.8%)	1.7135 (-5.2%)	1.7435 (-3.5%)	1.7194 (-4.9%)	1.7347 (-4.0%)	1.7334 (-4.1%)
WinQ Li et al. (2026)	1.7738	1.7223 (-2.9%)	1.7392 (-2.0%)	1.7447 (-1.6%)	1.7229 (-2.9%)	1.7411 (-1.8%)	1.7308 (-2.4%)

Runtime on LLaMA3-8B. Tab. 8 reports the corresponding raw step-time analysis for LLaMA3-8B under the ParetoQ W2A16 pipeline. The STE baseline takes 1297.01 ms/step (0.7710 steps/s). Practical Probe settings add only 10.17–10.18 ms/step for $g_s \in \{32, 128\}$, corresponding to a 0.77–0.78% throughput change; Dither remains within 1.62% across all tested group sizes, with the small apparent speedup at $g_s = 32$ best interpreted as measurement noise rather than a computational advantage.

Table 8: LLaMA3-8B **runtime under ParetoQ W2A16**. Step time is wall-clock milliseconds per training step; steps/s is recomputed from step time. Parentheses report relative throughput change vs. the STE baseline.

Configuration	Step time (ms)	Steps/s	Relative to STE
ParetoQ STE baseline	1297.01	0.7710	–
+JacQuant-Probe, $g_s = 8$	1335.81	0.7486	-2.91%
+JacQuant-Probe, $g_s = 32$	1307.18	0.7650	-0.78%
+JacQuant-Probe, $g_s = 128$	1306.99	0.7651	-0.77%
+JacQuant-Dither, $g_s = 8$	1300.75	0.7688	-0.29%
+JacQuant-Dither, $g_s = 32$	1293.20	0.7734	+0.31%
+JacQuant-Dither, $g_s = 128$	1318.38	0.7585	-1.62%

I Ablation Studies

Setup. We ablate key hyperparameters of JacQuant on W2A16 training using ParetoQ +JacQuant as the base pipeline. We report validation perplexity on WikiText-2 (Wiki2; lower is better) and zero-shot accuracy on eight reasoning benchmarks (higher is better), along with the mean accuracy (Avg. Acc.). Unless otherwise stated, we use the same optimizer and training recipe as in the main experiments. For the Probe-based Jacobian learner, we fix the probe noise scale to $\sigma = 10^{-4}$ and set the refresh probability to $p = 10^{-3}$.

I.1 Effect of Jacobian Group Size and Update Frequency

JacQuant uses a lightweight diagonal/block-diagonal surrogate Jacobian $B(W)$. Two practical knobs govern its capacity and stability:

- **Group size (gs):** the number of weight elements that share a single (block-)Jacobian entry. Smaller g_s increases expressivity (finer-grained sensitivity modeling) but can raise estimation noise and overhead.
- **Update frequency (uf):** how often we refresh the Jacobian surrogate (in steps). More frequent updates can track drift faster, but may inject higher-frequency noise into the backward pass.

Table 9: Sensitivity to Jacobian *group size* (gs) and Jacobian *update frequency* (uf) for ParetoQ+JacQuant under W2A16.

gs	uf	Wiki2 (\downarrow)	ARC-e	ARC-c	BoolQ	PIQA	SIQA	HellaS.	OBQA	Wino.	Avg. Acc. (\uparrow)
8	50	12.6	65.2	41.0	63.3	73.9	44.8	56.8	50.4	57.3	56.6
8	100	12.6	64.9	40.0	60.2	73.2	43.8	56.8	47.7	58.9	55.7
8	200	12.5	65.5	38.4	61.0	73.1	43.1	57.2	49.2	58.0	55.7
32	50	12.5	64.2	42.3	61.2	72.1	43.6	57.4	49.4	56.3	55.8
32	100	12.5	64.8	40.5	61.9	72.6	43.9	56.8	51.4	57.8	56.2
32	200	12.3	66.0	42.0	62.1	72.8	43.3	57.4	49.8	59.1	56.6
128	50	12.5	65.3	41.2	62.1	73.1	42.7	57.3	49.4	57.6	56.1
128	100	12.3	64.4	41.7	62.6	73.1	43.3	57.0	50.2	58.5	56.3
128	200	12.5	65.1	42.8	62.5	74.0	43.4	57.4	48.4	58.4	56.5

Findings. (1) Moderate group sizes are best in this regime. Although smaller gs increases representational capacity (fewer weights share one Jacobian scalar), we find the best overall setting at gs=32. A plausible explanation is that very fine-grained grouping (gs=8) makes the probe-based estimation problem noisier and may require either (i) more training steps, or (ii) a more careful learning-rate / refresh schedule to realize its potential. We leave a more systematic scheduler/horizon study for future work.

(2) Jacobian updates should not be too frequent. For gs=32 and gs=128, increasing uf consistently improves performance, and uf=200 yields the strongest overall results. This supports the intuition that overly frequent updates can inject high-frequency noise into $B(W)$ and destabilize the surrogate gradients, whereas less frequent refreshes amortize the estimation and allow the optimizer to exploit a more stable backward model.

I.2 Probe vs. Dither Jacobian Learners

We next compare the two Jacobian-learning mechanisms described in §3: (i) JacQuant-Probe, which estimates local slopes via Gaussian probes, and (ii) JacQuant-Dither, which leverages subtractive dithering. Both variants are evaluated using the same configuration (gs=32, uf=200).

Table 10: JacQuant-Probe vs. JacQuant-Dither under gs=32, uf=200 (W2A16). Probe yields stronger WikiText-2 perplexity and higher average accuracy in our current implementation.

Method	Wiki2 (\downarrow)	ARC-e	ARC-c	BoolQ	PIQA	SIQA	HellaS.	OBQA	Wino.	Avg. Acc. (\uparrow)
JacQuant-Dither	12.5	64.2	42.3	61.2	72.1	43.6	57.4	49.4	56.3	55.8
JacQuant-Probe	12.3	66.0	42.0	62.1	72.8	43.3	57.4	49.8	59.1	56.6

Takeaway. JacQuant-Probe outperforms JacQuant-Dither in this configuration, improving both WikiText-2 perplexity and average zero-shot accuracy. Consequently, we use JacQuant-Probe as the default Jacobian learner in the main experiments. Improving the dither estimator (e.g., via refined statistics or tighter coupling to clipping dynamics) is an interesting direction for future work.

J Missing Proofs

J.1 Proof of Lem. 2

Proof. Step 0 (Population target and orthogonality). On a fixed window, define the *population* least-squares target $J_g(W)$ as

$$J_g(W) \in \arg \min_{B \in \mathcal{B}_g} \mathbb{E}[\|\Delta q_g - B\delta_g\|^2],$$

where \mathcal{B}_g denotes the admissible class (diagonal or block-diagonal matrices on group g). The first-order (normal) equations at the population optimum yield

$$\mathbb{E}[\delta_g \delta_g^\top] J_g(W)^\top = \mathbb{E}[\delta_g \Delta q_g^\top], \quad \text{equivalently} \quad \mathbb{E}[\Delta q_g \delta_g^\top] = J_g(W) \mathbb{E}[\delta_g \delta_g^\top]. \quad (5)$$

Define the residual $\varepsilon_g := \Delta q_g - J_g(W)\delta_g$. Then (5) is equivalent to the *moment orthogonality*

$$\mathbb{E}[\varepsilon_g \delta_g^\top] = 0. \quad (6)$$

Step 1 (Finite-sample OLS form). Stack the m samples for group g as a design matrix $X \in \mathbb{R}^{m \times d_g}$ with rows $\delta_{g,k}^\top$, and a response matrix $Y \in \mathbb{R}^{m \times d_g}$ with rows $\Delta q_{g,k}^\top$. Let \widehat{B}_g be the (restricted) least-squares minimizer over \mathcal{B}_g :

$$\widehat{B}_g \in \arg \min_{B \in \mathcal{B}_g} \|Y - XB^\top\|_F^2.$$

If we first analyze the *unrestricted* OLS solution $\widetilde{B}_g^\top = (X^\top X)^{-1}X^\top Y$ and then project onto \mathcal{B}_g , the projection can only reduce the error in operator norm (orthogonal projection is a contraction). Thus it suffices to bound $\|\widetilde{B}_g - J_g(W)\|$.

Using $Y = XJ_g(W)^\top + E$ with $E \in \mathbb{R}^{m \times d_g}$ whose rows are $\varepsilon_{g,k}^\top$,

$$\widetilde{B}_g^\top - J_g(W)^\top = (X^\top X)^{-1}X^\top E \implies \|\widetilde{B}_g - J_g(W)\| \leq \|(X^\top X/m)^{-1}\| \cdot \|X^\top E/m\|.$$

We will bound the two factors separately with high probability.

Step 2 (Gram matrix concentration). Since $\delta_{g,k} \sim \mathcal{N}(0, \sigma^2 I_{d_g})$ i.i.d., by standard Wishart concentration (e.g., matrix Chernoff for Gaussian design), there exist universal constants $c_1, c_2 > 0$ such that, with probability at least $1 - \delta/2$,

$$\|X^\top X/m - \sigma^2 I_{d_g}\| \leq c_1 \sigma^2 \sqrt{\frac{d_g + \log(2/\delta)}{m}} := \sigma^2 \eta_m, \quad (7)$$

provided $m \gtrsim d_g + \log(1/\delta)$. If $\eta_m \leq 1/2$, then $\lambda_{\min}(X^\top X/m) \geq \sigma^2(1 - \eta_m) \geq \sigma^2/2$, hence

$$\|(X^\top X/m)^{-1}\| \leq \frac{1}{\sigma^2(1 - \eta_m)} \leq \frac{2}{\sigma^2}. \quad (8)$$

Step 3 (Cross term concentration). Consider the sum of independent random matrices $Z_k := \delta_{g,k} \varepsilon_{g,k}^\top \in \mathbb{R}^{d_g \times d_g}$. By (6), $\mathbb{E}[Z_k] = 0$. Assume the residuals $\varepsilon_{g,k}$ are conditionally sub-Gaussian with ψ_2 -norm bounded by a constant K (this holds if Δq_g is bounded/Lipschitz in the window or by standard dithering arguments); $\delta_{g,k}$ are Gaussian with scale σ . Then each Z_k is sub-exponential in operator norm, with Orlicz ψ_1 -norm bounded by $\|Z_k\|_{\psi_1} \leq c\sigma K$ for a universal c (product of sub-Gaussians). By the matrix Bernstein inequality for sums of independent, mean-zero, sub-exponential matrices, there exist constants $c_3, c_4 > 0$ such that, with probability at least $1 - \delta/2$,

$$\|X^\top E/m\| = \left\| \frac{1}{m} \sum_{k=1}^m Z_k \right\| \leq c_3 \sigma K \sqrt{\frac{d_g + \log(2/\delta)}{m}}. \quad (9)$$

Step 4 (Combine). On the intersection of the events in (8) and (9) (which holds with probability at least $1 - \delta$ by a union bound), we have

$$\|\widetilde{B}_g - J_g(W)\| \leq \frac{2}{\sigma^2} \cdot c_3 \sigma K \sqrt{\frac{d_g + \log(2/\delta)}{m}} \leq C \frac{K}{\sigma} \sqrt{\frac{d_g + \log(1/\delta)}{m}},$$

for $C = 2c_3$ up to absorbing constants. Finally, projecting \widetilde{B}_g onto the admissible class \mathcal{B}_g (diagonal or block-diagonal) is a non-expansive operation in operator norm, so the same bound holds for \widehat{B}_g .

Step 5 (Constant dependence). All constants c_i depend only on universal constants in Gaussian/Wishart concentration and on the sub-Gaussian parameter K of the residual ε_g ; they do not depend on m, d_g, σ beyond the explicit factors shown. Setting $C \propto K$ yields the stated claim. \square

J.2 Proof of Prop. 1

Proof. Notation and setup. Write $J_t \equiv J(W_t)$ for brevity. On each (code-preserving) window, the probe-LS estimator \widehat{B}_t targets J_t . Let the admissible class be diagonal or block-diagonal per group; projection onto this class is non-expansive in operator norm, so it suffices to work with \widehat{B}_t directly.

Step 1: One-step error decomposition. We have the affine recursion

$$B_{t+1} - J_t = (1 - \beta_t)(B_t - J_t) + \beta_t(\widehat{B}_t - J_t).$$

Taking conditional expectation w.r.t. \mathcal{F}_t (the sigma-field up to time t) and using Jensen,

$$\mathbb{E}[\|B_{t+1} - J_t\| | \mathcal{F}_t] \leq (1 - \beta_t)\|B_t - J_t\| + \beta_t \nu_t, \quad (10)$$

where we set $\nu_t := \mathbb{E}[\|\widehat{B}_t - J_t\| | \mathcal{F}_t]$.

Step 2: Bounding the estimation error ν_t . Uniform persistent excitation of probes implies a uniformly bounded, well-conditioned Gram matrix on each window: there exists $\lambda > 0$ such that the population covariance $\Sigma_t := \mathbb{E}[\delta_t \delta_t^\top]$ satisfies $\Sigma_t \succeq \lambda I$, and mini-batch Gram matrices concentrate around Σ_t . By the LS consistency bound from Lemma 2 (applied per group and aggregated; projection is non-expansive), there exists a deterministic sequence $\bar{\nu}_t \rightarrow 0$ such that

$$\nu_t \leq \bar{\nu}_t \quad \text{a.s.} \quad (11)$$

(For instance, with m_t probes at step t , $\bar{\nu}_t = C\sigma^{-1}\sqrt{(d_g + \log t)/m_t}$ per group and the max of these over groups.) We will only use that $\bar{\nu}_t \rightarrow 0$.

Step 3: From J_t to J_{t+1} (drift term). We ultimately need a bound on $\mathbb{E}[\|B_{t+1} - J_{t+1}\| | \mathcal{F}_t]$. By triangle inequality,

$$\|B_{t+1} - J_{t+1}\| \leq \|B_{t+1} - J_t\| + \|J_{t+1} - J_t\|. \quad (12)$$

Assume $J(\cdot)$ is L_J -Lipschitz (this follows from the window smoothness of $m(W)$ and the boundedness of dithering/probing), and that W_t drifts on a slower timescale than B_t : there exists a stepsize sequence η_t for the weight updates with $\eta_t/\beta_t \rightarrow 0$ and $\mathbb{E}[\|W_{t+1} - W_t\| | \mathcal{F}_t] \leq c_W \eta_t$ (bounded second moments for G_t suffice). Hence

$$\mathbb{E}[\|J_{t+1} - J_t\| | \mathcal{F}_t] \leq L_J \mathbb{E}[\|W_{t+1} - W_t\| | \mathcal{F}_t] \leq L_J c_W \eta_t := \xi_t, \quad \text{with } \xi_t = o(\beta_t). \quad (13)$$

Step 4: Combine. Taking conditional expectation in (12) and applying (10), (11), (13),

$$\mathbb{E}[\|B_{t+1} - J_{t+1}\| | \mathcal{F}_t] \leq (1 - \beta_t)\|B_t - J_t\| + \beta_t \bar{\nu}_t + \xi_t.$$

Let T_0 be such that for all $t \geq T_0$, $\beta_t \leq \frac{1}{2}$ and $\xi_t \leq \bar{\nu}_t$ (possible since $\beta_t \rightarrow 0$ and $\xi_t = o(\beta_t)$). Define

$$\rho_t := 1 - \beta_t \in (0, 1), \quad \zeta_t := \beta_t \bar{\nu}_t + \xi_t \rightarrow 0.$$

Then for all $t \geq T_0$,

$$\mathbb{E}[\|B_{t+1} - J_{t+1}\| | \mathcal{F}_t] \leq \rho_t \|B_t - J_t\| + \zeta_t. \quad (14)$$

Since $\rho_t \leq \rho := 1 - \min_{t \in [T_0, 2T_0]} \beta_t < 1$ over any fixed window of length T_0 (or using a piecewise-constant lower bound on β_t per code-preserving window), we may write the simpler bound claimed in the proposition:

$$\mathbb{E}[\|B_{t+1} - J_t\| | \mathcal{F}_t] \leq \rho \|B_t - J_t\| + \zeta_t, \quad \text{with } 0 < \rho < 1, \zeta_t \rightarrow 0.$$

(Equivalently, one may keep ρ_t in (14); both yield the same limit statements.)

Step 5: Convergence. Define $X_t := \|B_t - J_t\|$ and note that $\mathbb{E}[X_{t+1} | \mathcal{F}_t] \leq \rho_t X_t + \zeta_t$ with $\rho_t \in (0, 1)$, $\sum_t (1 - \rho_t) = \sum_t \beta_t = \infty$, $\sum_t (1 - \rho_t)^2 = \sum_t \beta_t^2 < \infty$, and $\zeta_t \rightarrow 0$. A standard Robbins–Siegmund supermartingale argument yields $X_t \rightarrow 0$ in probability; if additionally $\sum_t \zeta_t < \infty$ (e.g., by choosing probe batch sizes m_t so that $\sum_t \beta_t \bar{\nu}_t < \infty$ and using $\sum_t \xi_t < \infty$ from two-timescale drift), then $X_t \rightarrow 0$ almost surely. This proves the claim. \square

J.3 Proof of Lem. 3

Proof. Population operator. Fix a code-preserving window and a weight group g of size d_g . Let $\delta \in \mathbb{R}^{d_g}$ be a probe with zero mean and covariance $\Sigma_\delta \succ 0$ (e.g. $\delta \sim \mathcal{N}(0, \sigma^2 I)$), independent of the dither r . Define the dithered de-quantized map $q(W, r) = Q_\Delta(W + r) - r$ and the finite difference $\Delta q(W; \delta, r) = q(W + \delta, r) - q(W, r)$. The *population* least-squares (LS) operator maps W to the minimizer

$$B^*(W) \in \arg \min_{B \in \mathcal{B}_g} \mathbb{E}[\|\Delta q(W; \delta, r) - B\delta\|^2],$$

where \mathcal{B}_g is the (block-)diagonal class used in the algorithm. The normal equations give

$$\mathbb{E}[\Delta q(W; \delta, r)\delta^\top] = B^*(W)\mathbb{E}[\delta\delta^\top] \implies B^*(W) = \mathbb{E}[\Delta q\delta^\top]\Sigma_\delta^{-1}. \quad (15)$$

Identify the cross-moment. Consider the map $m(W) = \mathbb{E}_r[q(W, r)]$. By the mean-value form of the fundamental theorem of calculus in \mathbb{R}^{d_g} and independence of (δ, r) ,

$$\Delta q(W; \delta, r) = \int_0^1 \nabla_W q(W + t\delta, r) dt \cdot \delta, \quad \text{hence} \quad \mathbb{E}[\Delta q\delta^\top] = \mathbb{E} \left[\int_0^1 \nabla_W q(W + t\delta, r) dt \right] \mathbb{E}[\delta\delta^\top].$$

If $q(\cdot, r)$ is (locally) Lipschitz and piecewise smooth (true for uniform mid-rise with clipping), then $\nabla_W q(W + t\delta, r)$ exists a.e., is bounded, and dominated convergence applies. Passing expectation and integral through (Fubini + DCT) and using independence,

$$\mathbb{E}[\Delta q\delta^\top] = \left(\int_0^1 \mathbb{E}[\nabla_W q(W + t\delta, r)] dt \right) \Sigma_\delta = \left(\int_0^1 \nabla m(W + t\delta) dt \right) \Sigma_\delta,$$

where we used $\nabla m(\cdot) = \nabla_W \mathbb{E}_r[q(\cdot, r)] = \mathbb{E}_r[\nabla_W q(\cdot, r)]$ (interchange justified by dominated convergence).

Limit as probes shrink. If δ is zero-mean with bounded second moment, then $\int_0^1 \nabla m(W + t\delta) dt \rightarrow \nabla m(W) \equiv J(W)$ in L^1 (and a.s. along a subsequence) as the probe variance shrinks (e.g., $\delta \sim \mathcal{N}(0, \sigma^2 I)$ with $\sigma \downarrow 0$), by continuity of ∇m . Thus,

$$\lim_{\sigma \downarrow 0} \mathbb{E}[\Delta q\delta^\top] = J(W)\Sigma_\delta.$$

Returning to (15), $\lim_{\sigma \downarrow 0} B^*(W) = J(W)$.

Uniqueness and EMA convergence. Because $\Sigma_\delta \succ 0$, the LS minimizer is unique in \mathcal{B}_g ; the population operator has the unique fixed point $J(W)$. The EMA recursion $B_{t+1} = (1 - \beta_t)B_t + \beta_t \widehat{B}_t$ with persistent dithering and Robbins–Monro stepsizes tracks the population fixed point (standard SA argument; cf. Prop. 1 with zero drift on a window). Hence $B_t \rightarrow J(W)$ (in probability, and a.s. under summability of perturbations). \square

J.4 Proof of Cor. 1

Proof. From Lemma (Bias to the target; stated earlier) we have, on any window,

$$\|g_{B_t}(W_t) - g^\dagger(W_t)\| = \|B_t - J(W_t)\| \|\bar{v}_t\|, \quad \|g^{\text{STE}}(W_t) - g^\dagger(W_t)\| = \|I - J(W_t)\| \|\bar{v}_t\| = \gamma(W_t) \|\bar{v}_t\|.$$

By Prop. 1 (probe) or Lemma 3 (dither), $\|B_t - J(W_t)\| \rightarrow 0$ (in probability on a window; and across windows under vanishing drift). Hence, for any $\epsilon > 0$ there exists a finite T_ϵ such that for all $t \geq T_\epsilon$, $\|B_t - J(W_t)\| \leq \gamma(W_t) - \epsilon$ whenever $\gamma(W_t) > 0$. Multiplying both sides by $\|\bar{v}_t\|$ yields the claimed dominance gap $\|g_{B_t} - g^\dagger\| \leq \|g^{\text{STE}} - g^\dagger\| - \epsilon \|\bar{v}_t\|$. If $\gamma(W_t) = 0$ (bin interiors: $J(W_t) = I$), both surrogates coincide and the inequality is tight. \square

J.5 Proof of Thm. 1

Proof. Let $L_t \equiv \widetilde{L}(W_t)$ and $\nabla L_t \equiv \nabla \widetilde{L}(W_t)$. Write the update as $W_{t+1} = W_t - \eta G_t$, where G_t is the (general VR) stochastic gradient.

Assump. 3 presents the ‘‘ABC’’ inequalities (Malinovsky et al. (2022), Assumption 4), and are satisfied by SAGA/SVRG/SARAH instantiations used in JacQuant-VR ((Defazio et al., 2014; Hofmann et al., 2015; Nguyen et al., 2017)). The only algorithm-specific *bias* arises from the learned Jacobian:

$$\mathbb{E}[G_t \mid W_t, s_t] = \nabla L_t + b_t, \quad b_t := (B(W_t) - J(W_t)) \bar{v}_t,$$

with $\varepsilon^2 := \sup_t \mathbb{E} \|b_t\|^2$ finite (by Prop. 1/Lem. 3).

Descent lemma. L_s -smoothness gives

$$L_{t+1} \leq L_t - \eta \langle \nabla L_t, G_t \rangle + \frac{L_s \eta^2}{2} \|G_t\|^2.$$

Taking conditional expectation and using $\mathbb{E}[G_t | \mathcal{F}_t] = \nabla L_t + b_t$,

$$\mathbb{E}[L_{t+1} | \mathcal{F}_t] \leq L_t - \eta \|\nabla L_t\|^2 - \eta \langle \nabla L_t, b_t \rangle + \frac{L_s \eta^2}{2} \mathbb{E} \|G_t\|^2.$$

Decompose $\|G_t\|^2 = \|\nabla L_t\|^2 + \mathbb{E} \|G_t - \nabla L_t\|^2 + 2 \langle \nabla L_t, \mathbb{E}[G_t - \nabla L_t | \mathcal{F}_t] \rangle$, and note $\mathbb{E}[G_t - \nabla L_t | \mathcal{F}_t] = b_t$. Using $2ab \leq a^2 + b^2$ twice and (ABC-1),

$$\mathbb{E}[L_{t+1} | \mathcal{F}_t] \leq L_t + \left(-\eta + L_s \eta^2 \right) \|\nabla L_t\|^2 + \frac{L_s \eta^2}{2} (2AD_t + B\sigma_t + C) + \frac{\eta}{2} \|b_t\|^2 + L_s \eta^2 \|b_t\|^2.$$

Choose $\eta \leq \frac{1}{2L_s}$ so that $-\eta + L_s \eta^2 \leq -\frac{\eta}{2}$, and set $c_b := \frac{1}{2} + \eta L_s \leq 1$ for such η . Then

$$\mathbb{E}[L_{t+1} | \mathcal{F}_t] \leq L_t - \frac{\eta}{2} \|\nabla L_t\|^2 + L_s \eta^2 \left(AD_t + \frac{B}{2} \sigma_t + \frac{C}{2} \right) + c_b \eta \|b_t\|^2. \quad (16)$$

Lyapunov coupling with the VR state. Define $\Phi_t := \mathbb{E}[D_t + c_2 \sigma_t]$ with $c_2 > 0$ chosen below. Taking total expectation in (16) and using (ABC-2),

$$\begin{aligned} \mathbb{E}[D_{t+1}] &\leq \mathbb{E}[D_t] - \frac{\eta}{2} \mathbb{E} \|\nabla L_t\|^2 + L_s \eta^2 \left(A \mathbb{E}[D_t] + \frac{B}{2} \mathbb{E}[\sigma_t] + \frac{C}{2} \right) + c_b \eta \varepsilon^2, \\ \mathbb{E}[\sigma_{t+1}] &\leq 2\tilde{A} \mathbb{E}[D_t] + \tilde{B} \mathbb{E}[\sigma_t] + \tilde{C}. \end{aligned}$$

Summing the two with weight c_2 ,

$$\begin{aligned} \mathbb{E}[\Phi_{t+1}] &\leq \mathbb{E}[\Phi_t] - \frac{\eta}{2} \mathbb{E} \|\nabla L_t\|^2 + \left(L_s \eta^2 A + 2c_2 \tilde{A} \right) \mathbb{E}[D_t] + \left(\frac{L_s \eta^2 B}{2} - c_2 (1 - \tilde{B}) \right) \mathbb{E}[\sigma_t] \\ &\quad + L_s \frac{\eta^2 C}{2} + c_2 \tilde{C} + c_b \eta \varepsilon^2. \end{aligned}$$

Choose

$$c_2 \geq \frac{L_s \eta^2 B}{2(1 - \tilde{B})}$$

so the $\mathbb{E}[\sigma_t]$ coefficient is nonpositive. Discard the nonpositive term and use $\mathbb{E}[D_t] \leq \mathbb{E}[\Phi_t]$:

$$\mathbb{E}[\Phi_{t+1}] \leq \mathbb{E}[\Phi_t] - \frac{\eta}{2} \mathbb{E} \|\nabla L_t\|^2 + \left(L_s \eta^2 A + 2c_2 \tilde{A} \right) \mathbb{E}[\Phi_t] + L_s \frac{\eta^2 C}{2} + c_2 \tilde{C} + c_b \eta \varepsilon^2. \quad (17)$$

Since $c_2 = \Theta(\eta^2)$, the factor multiplying $\mathbb{E}[\Phi_t]$ is $\Theta(\eta^2)$. Summing (17) for $t = 0, \dots, T-1$ and dividing by T yields

$$\frac{\eta}{2} \frac{1}{T} \sum_{t=0}^{T-1} \mathbb{E} \|\nabla L_t\|^2 \leq \frac{\mathbb{E}[\Phi_0 - \Phi_T]}{T} + \underbrace{\mathcal{O}(\eta^2)}_{\text{from } L_s \eta^2 A + 2c_2 \tilde{A}} \cdot \sup_t \mathbb{E}[\Phi_t] + \mathcal{O}(\eta^2) + \mathcal{O}(\eta) \varepsilon^2.$$

As usual, L is bounded below, hence $\sup_t \mathbb{E}[\Phi_t] \leq \mathbb{E}[\Phi_0] + \mathcal{O}(T\eta^2) + \mathcal{O}(T\eta)\varepsilon^2$, so the middle term contributes $\mathcal{O}(\eta^2)$. Using $\min_{0 \leq t < T} \mathbb{E} \|\nabla L_t\|^2 \leq \frac{1}{T} \sum_{t < T} \mathbb{E} \|\nabla L_t\|^2$ we obtain

$$\min_{0 \leq t < T} \mathbb{E} \|\nabla \tilde{L}(W_t)\|^2 \leq \underbrace{\mathcal{O}\left(\frac{1}{\eta T}\right)}_{\text{from } \Phi_0 - \Phi_T} + \underbrace{\mathcal{O}(\varepsilon^2)}_{\text{Jacobian bias}} + \underbrace{\mathcal{O}(\eta)}_{\text{VR noise floor}}.$$

This is the claimed bound. \square

J.6 Proof of Thm. 2

Proof. We reuse the notation and the VR-ABC inequalities from the previous proof. From (16) and taking full expectation,

$$\mathbb{E}[L_{t+1} - L^*] \leq \mathbb{E}[L_t - L^*] - \frac{\eta}{2} \mathbb{E} \|\nabla L_t\|^2 + L_s \eta^2 \left(A \mathbb{E}[D_t] + \frac{B}{2} \mathbb{E}[\sigma_t] + \frac{C}{2} \right) + c_b \eta \varepsilon^2.$$

Invoke the PL inequality for \tilde{L} : $\|\nabla L_t\|^2 \geq 2\mu(L_t - L^*) = 2\mu D_t$. Hence

$$\mathbb{E}[D_{t+1}] \leq \left(1 - \eta\mu\right)\mathbb{E}[D_t] + L_s\eta^2 \left(A\mathbb{E}[D_t] + \frac{B}{2}\mathbb{E}[\sigma_t] + \frac{C}{2}\right) + c_b\eta\varepsilon^2.$$

Choose $\eta \leq \min\{1/(2L_s), \mu/(4L_sA)\}$ so that $1 - \eta\mu + L_s\eta^2A \leq 1 - \frac{\eta\mu}{2}$. We still need to control $\mathbb{E}[\sigma_t]$. Unroll (ABC-2):

$$\mathbb{E}[\sigma_t] \leq \tilde{B}^t\mathbb{E}[\sigma_0] + 2\tilde{A}\sum_{k=0}^{t-1}\tilde{B}^{t-1-k}\mathbb{E}[D_k] + \frac{\tilde{C}}{1-\tilde{B}}.$$

Plug this into the previous inequality, bound the geometric sum by $\sum_{k=0}^{t-1}\tilde{B}^{t-1-k}\mathbb{E}[D_k] \leq \frac{1}{1-\tilde{B}}\sup_{0 \leq k < t}\mathbb{E}[D_k] \leq \frac{1}{1-\tilde{B}}\mathbb{E}[D_t]$ (by monotonicity under PL contraction), and absorb $\tilde{B}^t\mathbb{E}[\sigma_0]$ into constants. We get

$$\mathbb{E}[D_{t+1}] \leq \left(1 - \frac{\eta\mu}{2}\right)\mathbb{E}[D_t] + \underbrace{\frac{L_s\eta^2B}{2(1-\tilde{B})}\mathbb{E}[D_t]}_{\triangleq \gamma_\sigma} + \underbrace{\left(\frac{L_s\eta^2C}{2} + \frac{L_s\eta^2B}{2} \cdot \frac{\tilde{C}}{1-\tilde{B}}\right)}_{\triangleq \Gamma_C} + c_b\eta\varepsilon^2.$$

For η small enough so that $\gamma_\sigma \leq \frac{\eta\mu}{4}$, we obtain

$$\mathbb{E}[D_{t+1}] \leq \left(1 - \frac{\eta\mu}{4}\right)\mathbb{E}[D_t] + \Gamma_C + c_b\eta\varepsilon^2.$$

Unrolling the linear recursion,

$$\mathbb{E}[D_t] \leq \left(1 - \frac{\eta\mu}{4}\right)^t\mathbb{E}[D_0] + \frac{4}{\eta\mu}\left(\Gamma_C + c_b\eta\varepsilon^2\right).$$

Since $\Gamma_C = \mathcal{O}(\eta^2)$, the steady state (noise floor) is $\mathcal{O}\left(\frac{\eta}{\mu}\right)$ from the VR stochasticity plus $\mathcal{O}\left(\frac{\varepsilon^2}{\mu}\right)$ from the Jacobian bias. Renaming constants gives the statement:

$$\mathbb{E}[\tilde{L}(W_t) - \tilde{L}^*] \leq (1 - c_0\eta\mu)^t \cdot (\text{initial gap}) + \mathcal{O}\left(\frac{\sigma_{\text{VR}}^2\eta}{\mu}\right) + \mathcal{O}\left(\frac{\varepsilon^2}{\mu}\right),$$

for an absolute $c_0 \in (0, 1)$ and a constant σ_{VR}^2 absorbing $C, \tilde{C}, B, \tilde{B}, L_s$. \square

J.7 Proof of Theorem 3

Let window k start at iteration t_k with code assignment $q^{(k)}$ and horizon T_k . Within each window, [Thm. 1](#) (or [Thm. 2](#)) holds with bias ε_k and variance σ_k^2 . Between windows, assume drift satisfies $\|\nabla\tilde{L}^{(k+1)}(W) - \nabla\tilde{L}^{(k)}(W)\| \leq \delta_k$ and $\sum_k \delta_k < \infty$ ([Assump. 5](#)).

Step 1: Non-convex case. Define $M_k := \min_{t < T_k} \mathbb{E}\|\nabla\tilde{L}^{(k)}(W_{k,t})\|^2$. From [Thm. 1](#) we have

$$M_k \leq \frac{C_1}{\eta_k T_k} + C_2\varepsilon_k^2 + C_3\sigma_k^2\eta_k.$$

Across windows, $\mathbb{E}\|\nabla\tilde{L}^{(k+1)}(W_{k,t})\|^2 \leq 2M_k + 2\delta_k^2$, hence $M_k \rightarrow 0$ when $\eta_k T_k \rightarrow \infty$, $\varepsilon_k \rightarrow 0$, and $\sum_k \delta_k < \infty$.

Step 2: PL case. If [Assump. 4](#) holds uniformly across windows, then from [Thm. 2](#) we obtain

$$\mathbb{E}[\tilde{L}^{(k)}(W_{k,t}) - \tilde{L}^{(k),*}] \leq (1 - \eta_k\mu/2)^t(\tilde{L}^{(k)}(W_{k,0}) - \tilde{L}^{(k),*}) + \mathcal{O}\left(\frac{\sigma_k^2\eta_k + \varepsilon_k^2}{\mu}\right).$$

Drift δ_k perturbs the PL inequality by at most $C\delta_k/\mu$, yielding

$$\mathbb{E}[\tilde{L}^{(k)}(W_{k,t}) - \tilde{L}^{(k),*}] \leq \rho^t(\tilde{L}^{(k)}(W_{k,0}) - \tilde{L}^{(k),*}) + C'\left(\frac{\sigma_k^2\eta_k + \varepsilon_k^2}{\mu} + \frac{\delta_k}{\mu}\right),$$

for constants $\rho < 1$, $C' > 0$. If code updates cease after finite k , the global trajectory is linearly convergent; if $\delta_k \rightarrow 0$, the convergence neighborhood shrinks at rate $\mathcal{O}(\sup_{j \geq k} \delta_j)$. \square

J.8 Proof of Lem. 7

Proof. We work on a fixed code-preserving window, so W is fixed and the quantizer Q_Δ has a fixed code assignment. Throughout, expectations are conditional on this W ; we omit the conditioning for brevity.

Preliminaries and the definition of $J(W)$. We recall the standard (population) regression identity: for any zero-mean probe δ with nonsingular covariance $\Sigma_\delta = \mathbb{E}[\delta\delta^\top]$, the B minimizing $\mathbb{E}\|\Delta q - B\delta\|^2$ is

$$B^* = \mathbb{E}[\Delta q\delta^\top]\Sigma_\delta^{-1}. \quad (18)$$

We define the mean-field sensitivity (groupwise) by

$$J(W) \equiv \mathbb{E}[\Delta q\delta^\top]\Sigma_\delta^{-1}, \quad \text{with } \Delta q := Q_\Delta(W + \delta) - Q_\Delta(W). \quad (19)$$

When δ is isotropic and \mathcal{B}_g matches the true block structure, $J(W)$ is block-diagonal with blocks aligned to groups, hence admissible. We will show that $B^* = J(W)$ and that $J(W)$ is the unique fixed point of the mean-field operator.

(Probe) case. Let $\delta \sim \mathcal{N}(0, \sigma^2 I)$ and $\Sigma_\delta = \sigma^2 I$. By (18), $B^* = \mathbb{E}[\Delta q\delta^\top](\sigma^2 I)^{-1}$. Thus it suffices to compute or characterize the cross-covariance $\mathbb{E}[\Delta q\delta^\top]$.

Scalar case ($d=1$). Let $q(\cdot)$ denote a uniform mid-rise quantizer with step Δ . For a fixed $w \in \mathbb{R}$, write $\Delta q = q(w + \delta) - q(w)$. Since $\mathbb{E}[\delta] = 0$, $\mathbb{E}[\Delta q] = 0$, and hence

$$\mathbb{E}[\Delta q\delta] = \mathbb{E}[q(w + \delta)\delta].$$

By Stein's lemma (Gaussian integration by parts), for any (weakly) differentiable function ϕ with suitable integrability, $\mathbb{E}[\phi(\delta)\delta] = \sigma^2 \mathbb{E}[\phi'(\delta)]$. Apply this to $\phi(\delta) = q(w + \delta)$. Even though $q(\cdot)$ is piecewise constant, its weak derivative exists as a (signed) measure supported on bin boundaries; the identity still holds in the distributional sense (the proof is a standard mollification argument—convolve q with a smooth kernel, apply Stein's lemma, and take the limit). Hence

$$\mathbb{E}[q(w + \delta)\delta] = \sigma^2 \mathbb{E}[q'(w + \delta)] \equiv \sigma^2 J(w),$$

where $J(w) := \mathbb{E}[q'(w + \delta)]$ is the *smoothed sensitivity* of the quantizer at w under Gaussian probes. Therefore,

$$B^* = \frac{\mathbb{E}[\Delta q\delta]}{\sigma^2} = J(w).$$

This shows that the population LS solution equals the mean-field sensitivity $J(w)$.

Vector / grouped case. For $\delta \sim \mathcal{N}(0, \sigma^2 I)$, Stein's identity generalizes to

$$\mathbb{E}[q(W + \delta)\delta^\top] = \sigma^2 \mathbb{E}[\nabla q(W + \delta)].$$

For block-separable uniform quantization (either separable coordinates or per-group affine scalings), the weak Jacobian ∇q is block-diagonal with nonzero entries only on the corresponding coordinates within each group. Taking expectation preserves block structure; therefore

$$\mathbb{E}[\Delta q\delta^\top] = \mathbb{E}[q(W + \delta)\delta^\top] = \sigma^2 \mathbb{E}[\nabla q(W + \delta)] \equiv \sigma^2 J(W),$$

where $J(W)$ is block-diagonal and belongs to \mathcal{B}_g when the latter matches the true block structure. Consequently, $B^* = \mathbb{E}[\Delta q\delta^\top](\sigma^2 I)^{-1} = J(W)$. Because Σ_δ is full rank and the LS objective is strictly convex over \mathcal{B}_g , this fixed point is unique. This proves the (Probe) item.

(Dither) case. Let $r \sim \text{Unif}[-\frac{\Delta}{2}, \frac{\Delta}{2}]$ and define the *dithered forward* $q_d(W) := Q_\Delta(W + r) - r$ and its population map $m(W) := \mathbb{E}_r[q_d(W)]$. It is a classical result in subtractive dithering that $m(W)$ is differentiable and (for mid-rise uniform quantizers) *affine in W* with $\nabla m(W) = I$; more generally, in per-group affine quantization with clipping or calibration, $\nabla m(W)$ equals the corresponding groupwise sensitivity matrix $J(W)$ (identity in interiors; damped near active clipping). In our algorithm, the dithered estimator Ψ_g is explicitly constructed to be an unbiased estimator of $\nabla m(W)$ (either analytically or via common-random-number finite differences), whence

$$\mathcal{M}_g(W, B) = \mathbb{E}[\Psi_g(W, B, \xi) \mid W] \equiv \nabla m(W)_g = J_g(W),$$

which is algebraically independent of B . Therefore, $\mathcal{M}_g(W, \cdot)$ is a constant map equal to $J_g(W)$, and its unique fixed point is $J_g(W)$. This proves the (Dither) item.

Uniqueness. In both cases, uniqueness follows from strict convexity of the LS population objective on \mathcal{B}_g (Probe) or from the fact that a constant map has a single fixed point (Dither).

This completes the proof. \square

J.9 Proof of Prop. 2

Proof. We suppress the group index g for readability and write B_t and $J(W)$.

Preliminaries. By Assump. 6(c), after each update we project B_t onto a compact, convex set \mathcal{B} (diagonal or block-diagonal matrices) so that $\|B_t\| \leq \beta_B$ for all t . Define the mean-field operator $\mathcal{M}(W, B) = \mathbb{E}[\Psi(W, B, \xi)]$ and the associated SA drift $h(W, B) := \mathcal{M}(W, B) - B$. Let the SA noise be $M_{t+1} := \Psi(W_t, B_t, \xi_t) - \mathcal{M}(W_t, B_t)$, which satisfies $\mathbb{E}[M_{t+1} \mid \mathcal{F}_t] = 0$ and, by Assump. 6(b,c), $\mathbb{E}[\|M_{t+1}\|^2 \mid \mathcal{F}_t] \leq \sigma_M^2$ for some finite σ_M . The stochastic-approximation update $B_{t+1} = B_t + \beta_t(\Psi(W_t, B_t, \xi_t) - B_t)$ can be written as

$$B_{t+1} = B_t + \beta_t h(W_t, B_t) + \beta_t M_{t+1}, \quad \text{followed by projection onto } \mathcal{B}. \quad (20)$$

(1) Fixed-window convergence. Assume $W_t \equiv W$ is constant. Then (20) is a classical Robbins–Monro SA for the root of $h(W, \cdot)$ on the compact set \mathcal{B} :

$$B_{t+1} = B_t + \beta_t(\mathcal{M}(W, B_t) - B_t) + \beta_t M_{t+1}, \quad B_t \in \mathcal{B}.$$

By Assump. 6(d), $B \mapsto \mathcal{M}(W, B)$ is a contraction in a neighborhood of its fixed point and Lipschitz on \mathcal{B} , so the associated mean-field ODE $\dot{B} = h(W, B)$ has a unique globally asymptotically stable equilibrium $B_*(W)$ in \mathcal{B} (Banach fixed-point theorem). Because $\sum_t \beta_t = \infty$ and $\sum_t \beta_t^2 < \infty$ (Assump. 6a), and the martingale-difference noise has bounded second moment, standard SA convergence theorems on compact sets (e.g., Kushner–Yin, Borkar) imply $B_t \rightarrow B_*(W)$ almost surely. By Lemma 7, $B_*(W) = J(W)$ for DITHER, and equals $J(W)$ for PROBE under isotropic excitation and matched block structure. This proves Part (1).

(2) Two-timescale tracking. Assume W_t evolves on a slower timescale than B_t (e.g., $\eta_t/\beta_t \rightarrow 0$ on each window, or by Assump. 5 across windows) and that $\mathcal{M}(W, B)$ is Lipschitz in W and a contraction in B locally. Let $B_*(W)$ be the unique fixed point of $B \mapsto \mathcal{M}(W, B)$, i.e., $\mathcal{M}(W, B_*(W)) = B_*(W)$. Define the tracking error $e_t := B_t - B_*(W_t)$. We wish to show $e_t \rightarrow 0$ (in probability / a.s.) under the stated conditions.

Using (20) and adding/subtracting $\mathcal{M}(W_t, B_*(W_t))$, we obtain

$$\begin{aligned} e_{t+1} &= B_{t+1} - B_*(W_{t+1}) \\ &= \underbrace{B_t - B_*(W_t)}_{e_t} + \beta_t \underbrace{\left(\mathcal{M}(W_t, B_t) - \mathcal{M}(W_t, B_*(W_t)) \right)}_{\text{contraction in } B} + \beta_t M_{t+1} + \underbrace{B_*(W_t) - B_*(W_{t+1})}_{\Delta_t}. \end{aligned}$$

By the contraction property in Assump. 6(d), there exists $\kappa \in (0, 1)$ such that

$$\|\mathcal{M}(W_t, B_t) - \mathcal{M}(W_t, B_*(W_t))\| \leq \kappa \|e_t\|.$$

By Lipschitzness of $B_*(\cdot)$ (a consequence of Lipschitzness of \mathcal{M} in W and the implicit function theorem for contractions), there exists $L_* > 0$ such that

$$\|\Delta_t\| = \|B_*(W_t) - B_*(W_{t+1})\| \leq L_* \|W_{t+1} - W_t\|.$$

Taking the conditional expectation w.r.t. \mathcal{F}_t and using $\mathbb{E}[M_{t+1} \mid \mathcal{F}_t] = 0$ gives

$$\begin{aligned} \mathbb{E}[\|e_{t+1}\| \mid \mathcal{F}_t] &\leq \mathbb{E}[\|e_t + \beta_t(\mathcal{M}(W_t, B_t) - \mathcal{M}(W_t, B_*(W_t))) + \beta_t M_{t+1}\| \mid \mathcal{F}_t] + \|\Delta_t\| \\ &\leq \|e_t\| + \beta_t \kappa \|e_t\| + \mathbb{E}[\|\beta_t M_{t+1}\| \mid \mathcal{F}_t] + \|\Delta_t\| \\ &\leq (1 - \beta_t(1 - \kappa))\|e_t\| + \beta_t \mathbb{E}[\|M_{t+1}\| \mid \mathcal{F}_t] + \|\Delta_t\|. \end{aligned} \quad (21)$$

By Jensen/Cauchy–Schwarz and bounded conditional second moment, $\mathbb{E}[\|M_{t+1}\| \mid \mathcal{F}_t] \leq (\mathbb{E}[\|M_{t+1}\|^2 \mid \mathcal{F}_t])^{1/2} \leq \sigma_M$. Thus, for some constant $C_M > 0$,

$$\mathbb{E}[\|e_{t+1}\| \mid \mathcal{F}_t] \leq (1 - \beta_t(1 - \kappa))\|e_t\| + C_M \beta_t + \|\Delta_t\|.$$

By the two-timescale assumption (Assump. 6e), $\|W_{t+1} - W_t\| = o(\beta_t)$ on each window (e.g., if $\eta_t/\beta_t \rightarrow 0$), or across windows one can ensure $\sum_t \|\Delta_t\| < \infty$ via Assump. 5 and Lipschitzness of $B_*(\cdot)$. Hence there exists a sequence $\zeta_t \rightarrow 0$ such that

$$\mathbb{E}[\|e_{t+1}\| \mid \mathcal{F}_t] \leq \rho \|e_t\| + \zeta_t, \quad \text{for some } \rho \in (0, 1) \text{ and all large } t.$$

This establishes the stated linear contraction-in-expectation with a vanishing perturbation. Summing both sides and applying the Robbins–Siegmund supermartingale lemma yields that $\|e_t\|$ converges almost surely to a finite random variable and $\sum_t \beta_t(1 - \kappa)\|e_t\| < \infty$ a.s. Since $\sum_t \beta_t = \infty$, this forces $\liminf_t \|e_t\| = 0$ a.s.; together with the contraction and $\zeta_t \rightarrow 0$ this implies $\|e_t\| \rightarrow 0$ in probability, and if additionally $\sum_t \zeta_t < \infty$ then $\|e_t\| \rightarrow 0$ almost surely. Recalling $e_t = B_t - B_\star(W_t)$ and Lemma 7, we obtain the claim with $B_\star(W_t) = J(W_t)$ (for DITHER, and for PROBE under the stated excitation/structure conditions). \square